5-2016

# Analytical Evaluation of an Atmospheric Pressure Glow Discharge Microplasma as an Emission Source

Sarah M. Harris
*Clemson University*, chemist.sarah.90@gmail.com

# ANALYTICAL EVALUATION OF AN ATMOSPHERIC PRESSURE GLOW DISCHARGE MICROPLASMA AS AN EMISSION SOURCE

---

A Thesis
Presented to
the Graduate School of
Clemson University

---

In Partial Fulfillment
of the Requirements for the Degree
Master of Science
Chemistry

---

by
Sarah M. Harris
May 2016

---

Accepted by:
Dr. R, Kenneth Marcus, Committee Chair
Dr. George Chumanov
Dr. Brian Powell

# ABSTRACT

In scenarios such as environmental contamination or on-site nuclear analysis, an instrument capable of rapid, in-field chemical analysis would be faster and more cost-effective than the current practice of sending samples back to the laboratory for analysis. An ideal instrument for this purpose will consume little power, produce a small footprint, use small sample volumes with no sample preparation, produce no waste, and operate in ambient conditions while maintaining the high precision and accuracy needed to make time-sensitive decisions.

The liquid sampling-atmospheric pressure glow discharge (LS-APGD) microplasma, developed by Marcus and co-workers, is a novel excitation source for atomic emission spectroscopy developed to meet these goals. This emission/ionization source meets the demands needed for field-capable instrumentation by being cost efficient and having a small footprint, low power consumption, high salt/matrix tolerance, and little to no waste production. The microplasma is generated in a 1-2 mm gap sheathed in a helium gas between a stainless steel electrode and an electrolytic solution. Since its conception, the LS-APGD has been used for a variety of sample mediums (e,g,, liquid, solid, and laser ablated particles) and as an elemental and an organic ionization source, and as an emission source for detection by mass spectrometry (MS) and optical emission spectroscopy (OES), respectively.

Previous research employing the LS-APGD microplasma has assessed optimized components and operating parameters for multiple sample introductions and methods of detection. This work presents an analytical study of the LS-APGD microplasma as an

emission source for solution samples. The goal of this research is to illustrate the capabilities of this emission source by quantitative assessment. An evaluation of the source in terms of line selection and theoretical limits of detection progresses the microplasma towards successful implementation while the analysis of matrix effects unveils broader capabilities of analysis and deeper understanding of the source. This characterization and examination of the LS-APGD microplasma, combined with past assessments, illustrates the potential of this source as a portable instrument for in-field elemental spectroscopy.

# DEDICATION

I would like to dedicate this thesis to all those who strengthened and helped me along the way. To my friends at Clemson, for all the adventures, and for going through this journey with me. I would not have wanted to do any of this without you. Specifically to Paul, for your companionship, your unfailing friendship, and your empathy through everything. My graduate school experience was better for having you in it. To Kelly Crawford at the ADFS for all her imparted wisdom. To Tori, for understanding my frustrations without me saying a word, and for always being there for me, no matter what.

To Phoebe for being there during every late night and every early morning, with ample enthusiasm and support. Friedrich Ferdinand Runge, for his original isolation of caffeine.

To those who believed in me, and especially for those who did not for providing me the opportunity to prove you so very, very wrong.

To my family, thank you for your love and support through this process. I have appreciated every encouraging text and scientific discussion you have granted me, every encouraging word along the way, and for knowing I could do it. Specifically to Mom and Dad, thank you for nurturing my love of science, for your love and support, and for believing in me when I didn't believe in myself.

# ACKNOWLEDGMENTS

I would like to acknowledge those who have contributed to my scientific knowledge and enthusiasm over the years. Mrs. Schonoff from Grissom High School, for making chemistry exciting and enjoyable. To the devoted professors at the University of Alabama in Huntsville who answered my questions, taught me so much, and encouraged my confidence in science, especially Dr. and Mrs. William and Mary Setzer, for encouraging me to tutor and to readily discuss science will peers and colleagues. You showed me how much you learn by teaching and how practical and exciting chemistry can be. I will never forget how you both go above and beyond to assist a student in learning more. To Drs. Rob and Hana McFeeters, for allowing me to experience research, your unconditional support, and for letting me learn without being afraid to fail. I was truly blessed to research in your laboratory.

I would also like to acknowledge those I had the opportunity to learn from along the way including Dr. Koppenaal, Dr. Barinaga, Dr. Hart, and Dr. Haber for your imparted wisdom and friendship.

I would like to acknowledge those at Clemson University for their time, efforts, and dedication. My advisor, Dr. Marcus, for providing me the opportunities for personal and professional growth. To the other members of the Marcus group, past and present, you have enriched my experience and taught me so much. I am eternally grateful for our group lunches, for working through difficult problems with me, and for being right there alongside me.

TABLE OF CONTENTS

Page

Table of Contents (Continued)

Page

LIST OF TABLES

LIST OF FIGURES

List of Figures (Continued)

Page

List of Figures (Continued)

Page

# CHAPTER ONE

# INTRODUCTION

After the preliminary proof of concept of novel instruments or methods and initial operating parameter investigation, an assessment of the instrument or method in terms of capability and comparison to current techniques must be accomplished before commercialization and general acceptance can occur[1]. Assessment of a new chemical technique, method, or instrument requires evaluation using a wide range of parameters which include precision, reproducibility, repeatability, accuracy and bias, capability of detection, and ruggedness[1]. Precision, as defined by International Organization for Standardization (ISO), refers to the "distribution of a result and may be evaluated through uncertainty, repeatability [obtaining the same results using the same testing methodologies by the same operator, equipment, or in a short time scale], or through reproducibility [obtaining the same result using the same testing methodologies by different operators, equipment, or over a long time scale]"[2]. Accuracy and bias evaluate the closeness of method response of a single measurement to the true value and is evaluated by comparison to certified reference materials similar to the future expected sample compositions[2]. Capability of detection is evaluated through assessment of limit of detection (LOD) and limit of quantification (LOQ) which are the concentrations at which an analyte can be reported with a specified degree of certainty as detected and be quantified, respectively[3]. The capability of detection includes evaluation of the dynamic range which is an assessment of the lowest and highest detection concentrations of an analyte using a linear or constant calibration slope[3]. Ruggedness, or robustness, refers to

the range of parameters of operation or to the variety of samples and matrices which can be analyzed[1]. Other instrumental considerations may include the expected knowledge base of the operator, the frequency of use and maintenance, and the physical requirements of power, consumables, waste production, etc. The target objectives for validation when designing new instruments are always specific to the motivations for the research created by the need or gap in technologies, such as the International Target Values for instruments accepted for nuclear materials measurements written by the International Atomic Energy Agency (IAEA)[4].

The need for rapid chemical analysis in the field is the principal motivation of the investigation into portable instrumentation. There are focused efforts to develop portable, in-field instruments in for atmospheric pollutant monitoring[5], healthcare[6] , and nuclear forensics[7]. In scenarios where prompt, on-site results are necessary, such as environmental contamination, in-space analysis[8], or on-site nuclear forensics, an instrument capable of rapid, in-field chemical analysis would improve efficiency and response time because of real-time feedback which limits sample handling and transport back to laboratories. Atomic analysis is one specific region of field-deployable instrumentation with a specific interest and need for development[9-11]. In these environments, optical emission spectroscopy (OES) can provide confident and rapid elemental analysis. OES detection uses an excitation source to excite electrons to a higher energy level specific to each atom. The energy released upon relaxation is equal to the energy difference between the atom's specific quantized orbital energy levels which is emitted in the form of photons. The photons propagate at wavelengths in the ultraviolet

and visible spectral regions. This emitted light is collected and focused through optical components and delivered to a spectrometer containing a detection system such as a photomultiplier tube (PMT), photodiode array (PDA), or charge-coupled device (CCD).

For an OES instrument to be easily implemented as a field-capable device, the instrument must have a small footprint, require minimal power, need few consumables such as gas or solvent, and produce minimal waste. To meet these requirements, the instrument must be able to operate in ambient conditions to eliminate the need for a vacuum pump. An instrument for this application must provide rapid results and be user friendly with simple required maintenance. In terms of the validation parameters, an *ideal* field-capable instrument would match the precision and accuracy of the present laboratory-based analysis to eliminate the need to bring the sample to the laboratory entirely. It would also have low LODs and LOQs, be capable of analysis over a broad linear range, and be able to analyze multiple sample matrices.

The established method for present day laboratory-based elemental analysis is the inductively coupled plasma (ICP) detected by OES or mass spectrometry (MS)[8,12-14]. ICP-OES/MS has a broad dynamic range for multi-element detection with high sensitivities (i.e. low LODs) and the ability to handle a large number of samples each day. Commercially introduced in 1983, the ICP-MS is a robust instrument is capable of detecting more than 70 elements and sets the bar for elemental detection[14]. Liquid samples are introduced into a nebulizer by use of a peristaltic pump to form an aerosol of droplets due to the application of a high flow-rate gas, such as Ar. The aerosol samples are then introduced to a spray chamber where the heavier droplets are removed and fine

droplets become dry particles as the solvent evaporates. The dry particles become introduced into the plasma for atomization/excitation/ionization. The plasma is generated from the establishment of an electromagnetic field from a radio frequency power supply on to a large volume (16 L $min^{-1}$) of Ar gas. The electromagnetic field ionizes the Ar resulting in a stable, high temperature plasma between 7000 to 8500 K as a result of the inelastic collisions generated between neutral Ar atoms and the charged particles[15]. From there, in ICP-MS, the ions of the sample generated in the plasma are directed through a mass spectrometer which sorts the ions according to mass-to-charge ratio before detection. In ICP-OES, the light emitted from the plasma as a result of the excited analyte particles is collected and separated into its discrete component wavelengths using a diffraction grating before being detected by a multichannel detector (e.g. PDA, CCD) for simultaneous detection of the dispersed spectrum. As good as the figures of merit of an ICP-OES/MS are, the instrument is prevented from portable analysis due to its high power requirements (1-2 kW), large gas requirements (up to 16 L $min^{-1}$), solvent volumes (1-2 mL $min^{-1}$), and periphery equipment (e.g. exhaust vent, vacuum pumps, waste containment).

In an effort to miniaturize, research into smaller ionization and emission sources such as glow discharges, and microplasmas, grew rapidly[11,16,17]. In the early 1990s, Cserfalvi *et al.* developed an electrolyte cathode discharge (ELCAD) that employs an electrolytic solution as one discharge electrode for plasma generation in atmospheric conditions[18]. The utilization of an electrolytic solution as a discharge electrode enables uninterrupted delivery of liquid samples into the plasma for elemental analysis. In

ELCAD devices, the electrolytic solution flows (2-10 mL $min^{-1}$) upwards through a vertically-mounted glass tube before overflowing into a catch basin. A counter electrode (anode) is placed three to five millimeters above the cathode. A d.c. voltage (<1 kV) is then applied to sustain a plasma between the solution surface and the counter electrode. The creation of the ELCAD prompted a surge of interest into modified emission sources which continues today[19-21]. A miniaturized and improved-upon version of the ELCAD was developed by Hieftje, and co-workers called the solution-cathode glow discharge (SCGD)[22,23]. Using essentially the same electrode design, but with a lower-flow rate (2.5-3.5 mL $min^{-1}$), it allows for injections of 25 µL sample volumes with improved upon, sub µg $L^{-1}$ detection limits.

With the goal of a portable instrument in mind, and the associated validation parameters, Marcus and Davis introduced the liquid sampling-atmospheric pressure glow discharge (LS-APGD) microplasma as an alternative to the existing emission sources designed with an electrolytic solution acting as an electrode[24-27]. The most significant difference between the LS-APGD and other ELCAD-type plasmas is the ability to operate in a total-consumption mode due to a high power density (>10 W $mm^{-1}$) nd a lower solution flow rate; therefore, generating no waste. The LS-APGD utilizes the electrolytic flow emerging from a metal capillary at rates from 10-300 µL $min^{-1}$, as designated optimal for the method of detection employed. The electrolytic solution acts as an electrode emerging from a concentric metal capillary which carries a flow of cooling/sheath gas (e.g. Ar, He, or $N_2$) at low gas flow rates (0.1- 1 L $min^{-1}$) around the solution-containing capillary. This solution electrode is placed two millimeters or less

across from a metal counter electrode (Cu, Ni, or stainless steel) to sustain a glow discharge plasma at the liquid surface. A diagram of the LS-APGD set up for OES is seen in Fig. 1.1. The LS-APGD has been employed for optical emission spectroscopy[24] as well as organic[28] and inorganic[29] MS[30] analysis to collect isotopic, elemental, and molecular information. Multiple samples types have been analyzed including liquids, solids, and laser-ablated samples [29,31,32].

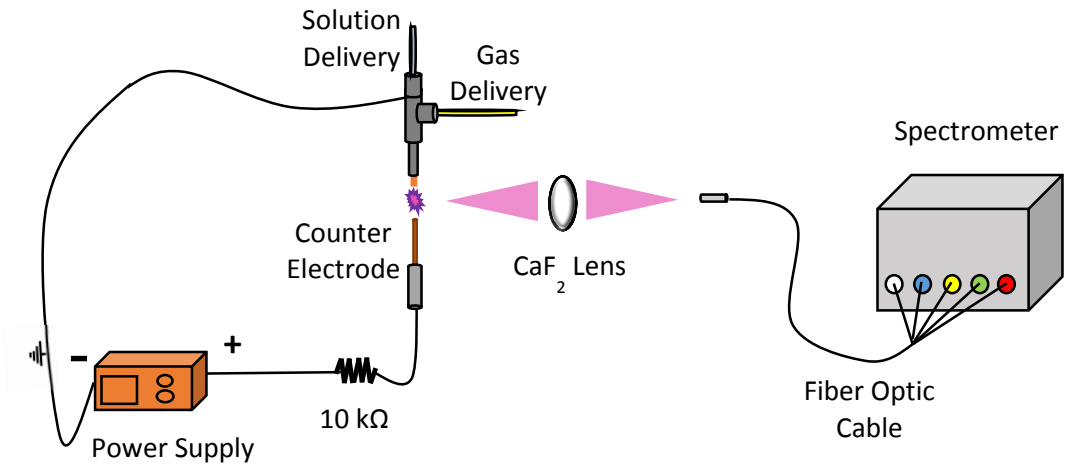


**Figure 1.1 Depiction of LS-APGD-OES. Microplasma is generated between the counter electrode and the solution electrode. The emission light is collected by the $CaF_2$ lens and delivered to the spectrometer by the fiber optic cable.**

Previous work has explored proof of concept and initial operating parameters, setting the stage for analytical assessment. Recent studies have focused on inter-parametric studies for OES[33] and MS[30], and investigation of plasma temperature characteristics, plasma robustness [34] for greater insight to the sample analysis mechanisms (i.e. capability and processes of excitation/ionization) of the LS-APGD[28]. As a novel excitation source, the instrument parameters of precision, reproducibility,

repeatability, accuracy and bias, capability of detection, and ruggedness are under investigation. To continue the development of the LS-APGD microplasma as an emission source for field-capable spectroscopic analysis, this work investigates the instrument parameters of precision, detection capability, and ruggedness through methodological line selection, detection limit determination, and examination of matrix effects, the results of which are presented in Chapter Two and Chapter Three.

# CHAPTER TWO

# LINE SELECTION AND FURTHER CHARACTERIZATION OF THE LIQUID SAMPLING-ATMOSPHERIC PRESSURE GLOW DISCHARGE (LS-APGD) FOR OPTICAL EMISSION SPECTROSCOPY


## Abstract

A methodical approach to line selection using signal-to-background (S/B) ratios and signal-to-noise (S/N) ratios has been carried out, along with an evaluation of limits of detection (LOD) using the liquid sampling-atmospheric pressure glow discharge (LS-APGD) microplasma as an excitation source for optical emission spectroscopy (OES). The LS-APGD emission source was monitored using a spectrometer composed of a five-channel, charge-coupled device (CCD) array allowing for the simultaneous acquisition of spectra from 190-884 nm. Ten elements, Ag, Cs, Cu, Li, Mg, Na, Ni, Pb, U, and Zn, are employed in the evaluation due to their utility for understanding the plasma and for their prevalence as analytes of interest for in-field analysis. While work remains with regards to plasma and emission optimization, it is believed that the LS-APGD has significant potential to facilitate lower-cost, simple, and transportable optical emission spectroscopy.


## Introduction

In the realm of analytical chemistry, there is a focused effort to develop portable, in-field instruments in areas such as monitoring of environmental contamination[5], healthcare[6], and nuclear forensics[7]. In scenarios such as environmental contamination or on-site nuclear analysis, an instrument capable of rapid, in-field chemical analysis would be more efficient and responsive than the current practice of delivering samples from the

field to a laboratory for analysis, saving valuable time and resources. This is especially pertinent when the sample cannot be sent back to the lab due to the presence of hazardous materials, radioactivity, or unknown materials. The forerunner for in-laboratory instrumentation of atomic analysis, particularly emission analysis, is inductively coupled plasma-optical emission spectrometry (ICP-OES). Though robust and powerful, the ICP-OES is limited to laboratory analysis due to the requirement for high power input and the need for a large supply of Ar gas. The investigation into miniaturized instrumentation has been pursued since the 1970s, not just for portability, but also to reduce the cost of analysis by decreasing the consumables required[35]. Examples of the research into miniaturization can be seen in the reviews on miniature mass spectrometers[36] or specific portable instruments for medical, imaging, and diagnostic purposes[37,38]. Such an instrument must consume little power, have a small footprint, require small sample volumes with minimal dilution, digestion, or further addition of solvents, and operate in ambient conditions. To this end, the field of research into smaller ionization and emission sources such as glow discharges, and microplasmas, has seen appreciable growth[11,16,17].

One promising area of investigation, glow discharge (GD) plasmas, involves the development of plasmas which employ an electrolytic solution as one of the discharge electrodes. These devices fall into the group of atmospheric pressure glow discharges (APGD). The concept demonstrated by Cserfalvi and co-workers was called the electrolyte cathode discharge, or ELCAD[18]. In ELCAD devices, an electrolytic solution, which also contains the analyte, is delivered through a vertically-mounted glass tube between 2-10 mL $min^{-1}$, overflowing into a catch basin, generating a continuous

waterfall. An electrode is placed three to five millimeters above this constant solution stream, and is connected to the ground output of a d.c. power supply, sustaining a plasma between the solution surface and the counter electrode. Initial analytical sensitivities were demonstrated with linear response curves from 1-50 μg $mL^{-1}$ [18]. Since the initial description, investigation into modified emission sources designed with an electrolytic solution acting as an electrode has expanded dramatically and continues today[19-21]. One of the sources employed after the description of the ELCAD was a miniaturized version developed by Hieftje, and co-workers[22,23]. Using essentially the same electrode design, which they called the solution-cathode discharge (SCD), but with a lower-flow operating space, the devices operated at flow rates of 2.5-3.5 mL $min^{-1}$, allowing injection of 25 μL sample volumes with sub μg $L^{-1}$ detection limits.

As an alternative to the high waste production and acidic solution pool of the ELCAD, Marcus and co-workers introduced the liquid sampling-atmospheric pressure glow discharge (LS-APGD) microplasma[24-27]. The most significant difference between the LS-APGD and the ELCAD is in the electrolytic flow. Instead of a fountain that flows into a pool, the LS-APGD utilizes the electrolytic flow emerging from a fused-silica capillary at a wide range of flow rates, but all less than 300 μL $min^{-1}$, allowing for total consumption. The electrolytic solution acts as an electrode emerging from a concentric metal capillary carrying a flow of cooling/sheath gas (e.g. Ar, He, or $N_2$) at low gas flow rates, less than 1 L $min^{-1}$, around the solution containing capillary. This solution electrode is placed across from a metal counter electrode (Cu, Ni, or stainless steel) separated by a distance of two millimeters or less to sustain a GD microplasma at the liquid surface. The

LS-APGD physical set-up has been shown to be versatile in meeting the need for analyzing different sample forms (e.g. liquids, solids, particles) and for pairing with a variety of detection systems when gathering elemental, isotopic, and/or molecular information[28,31,33]. To date, the LS-APGD has been employed for optical emission[24] and mass spectrometric[30] analysis, organic[28] and inorganic[29] determinations, for liquids and laser-ablated samples[31]. Recent studies have focused on the investigation of plasma temperature characteristics, plasma robustness[34], and an inter-parametric relationships as both an emission[33] and as an ionization source[30] providing greater insight to the working mechanisms and atomic physics of the LS-APGD[28].

The spectrometer selected for detection in these studies is the Aurora spectrometer (Applied Spectra, Inc., Fremont, CA, USA) controlled by 'Aurora' Data Analysis Software. The Aurora software allows for the monitoring of emission spectra, identification of emission peaks for the elements, correction of background signal, and integration of the atomic and ionic emission peak areas. This instrument provides the option to use a laptop, rather than a desktop with more computing power, for data collection, data analysis, and spectrometer control, allowing for small physical system requirements of the spectrometer. This 15 pound, compact (9.5" length x 10" width x 7" height) spectrometer is a practical candidate for future portable detection of the LS-APGD given the balance between detection sensitivity and spectral resolution (<0.1 nm) and stated physical attributes. Aside from the small physical dimensions, the system requires 120/220 VAC, 50/60 Hz and less than 2A. Put into perspective, this is the power requirement, in wattage, of a household blender[39]. Along with the spectrometer,

additional LS-APGD components have been chosen for use based on their small size, power, and weight parameters. These choices complement the emission source in its minimal consumption sustaining liquids and discharge gas, as well as its lack of waste production since it operates in a total consumption mode.

To advance the development of the LS-APGD for OES towards practical in-field use, it is important to provide a methodical line selection among the many atomic and ionic transitions that can be observed. Along with a discussion of the line selection for the elements Ag, Cs, Cu, Li, Mg, Na, Ni, Pb, U, and Zn, an evaluation of the current theoretical analyte limits of detection (LODs) for emission detection using the Aurora spectrometer is presented here. It is widely known that the signal to noise ratio, signal to background ratio, and signal intensities vary from line to line for each element due to the strength of the electronic transitions and the background signal at those wavelengths[40]. As with any developed optical analysis technique, successful implementation of the LS-APGD-OES relies on the methodical choice of the optimal set of elemental transitions based on detailed evaluations of signal-to-noise, signal-to-background, reproducibility, and LODs.

## Experimental Setup

### *LS-APGD source*

In these studies, the LS-APGD microplasma source was sustained between an electrolytic test solution (500 mg $L^{-1}$ X where X is the analyte of interest in 2% $HNO_3$) and stainless steel high voltage electrical feedthrough (304 SS, 1 kV, MDC Vacuum

Products, LLC, Hayward, California, USA) that functions as the counter electrode. The electrolytic solution was introduced through a fused-silica coated metal capillary (280 mm i.d., 580 mm o.d., Restek Corporation, Bellefonte, PA, USA) housed concentrically within in a hollow, stainless steel capillary (316 SS, 0.8 mm i.d., 1.6 mm o.d., IDEX Health and Science, Oak Harbor, WA, USA). This gas/liquid introduction assembly was secured to a translational stage (460PXYZ, Newport Corporation, Irvine, CA, USA) used to align the electrode co-linearly (i.e. 180° geometry) with the counter electrode. A continuous electrolytic flow of 150 µL $min^{-1}$ 2% $HNO_3$ was maintained by means of a syringe pump (NE-1000, New Era Pump Systems, Inc., Farmingdale, NY, USA), found to be the optimal flow rate for emission studies in previous research[33]. Discrete injections of analyte were made using an injection valve (Rheodyne Manual Sample Injector Valve 7725i, Sigma-Aldrich Inc., St. Louis, MO, USA) supplied with a 50 µL injection loop. The He sheath gas was introduced between the capillary and the sheath gas electrode and regulated by a mass flow controller (0-1 SLPM, Alicat Scientific, Inc., Tucson, AZ, USA), connected to a gas line from the primary He source by means of a tee-piece (Swagelok, Solon, OH, USA).

The microplasma was sustained by a high voltage power supply (3 kV, 0–200 mA, SL3PN600, Spellman High Voltage Electronics Corporation, Hauppauge, NY, USA) operating in the constant current (d.c.) mode with a negative voltage output. A ballast resistor (10 kΩ, 300 W, Arcol Ltd UK, Truro, Cornwall, England, UK) was placed in-line between the power supply and the solution introduction electrode (anode), while the counter electrode was held at ground potential (cathode), as this has been shown to be

the most advantageous powering mode[26]. High voltage delivery and small inter-electrode distances have been shown to produce the best emission signal from solution delivered analytes due to generation of the highest plasma power densities[33]. Photographic images of the LS-APGD-OES set-up as well as diagrammatic representations of the source can be found in previous publications[26,33].

*Optical emission spectrometer*

A five-channel, broad wavelength optical spectrometer (Aurora, Applied Spectra, Inc., Fremont, CA, USA) was used to detect the optical emission signal from the microplasma. The spectrometer, equipped with a CCD linear array detector module, allows for the simultaneous acquisition of spectral wavelengths from 190 to 884 nm. LS-APGD microplasma emission was collected by focusing the entirety of the plasma image by means of a biconvex $CaF_2$ lens (25.4 mm diameter, 50.0 mm focal length, Thorlabs, Inc., Newton, NJ, USA) onto a multi-channel optical fiber bundle which conveyed the emission to the separate spectrometer channels. When using any optical lens system, chromatic aberration, the failure of the optics to bring all the wavelengths collected into focus at the same convergence point, must be considered. Though chromatic aberration can be avoided by use of a mirror, this system was designed with a lens instead of a mirror in efforts to limit spatial requirements in the development of a compact field-capable emission analysis system while maintaining significant light collection. The lens was mounted by means of optomechanical cage system components (Thorlabs, Inc., Newton, NJ, USA) on a translational stage (460P-XYZ, Newport Corporation, Irvine, CA, USA) to allow for spatial optimization by movement on the x-axis of the distance

from the lens to the microplasma. The distance from the plasma to the lens, as well as the lens to the fiber optic cable, was set such that the whole plasma emission was projected upon the fiber optic bundle (1:1). This distance was proportional to the electrode gap such that any alteration in the maximum lateral plasma dimension required alteration of the lens positioning to maintain deliverance of the entirety of the plasma excitation production on to the fiber optic cable for detection. Data acquisition was accomplished using the 'Aurora' Data Analysis Software (Applied Spectra, Inc., Fremont, CA, USA). Individual spectra (190 to 884 nm with spectral resolution < 0.1 nm) were collected over a predetermined time using an integration time of 1.05 ms at a repetition rate of 10 Hz.

*Spectral data processing*

Spectra acquired in the 'Aurora' Data Analysis Software were read into MatLab (MATLAB 8.0 and Statistics Toolbox 8.1, The MathWorks, Inc., Natick, MA, USA.) for further data processing. The final signal evaluated for each analyte was the integration of signal intensity over the wavelengths spanning from the signal onset to the return to baseline of the given transition. This is demonstrated in Fig. 2.1 in the spectral region from 322-332 nm for a Cu solution. Within the figure the marker '1' indicates the initial pixel of integration while the marker '2' indicates the pixel at which integration ends. For the background measurements used in statistical evaluation the same pixels were selected for beginning and ending integration in the absence of analyte.

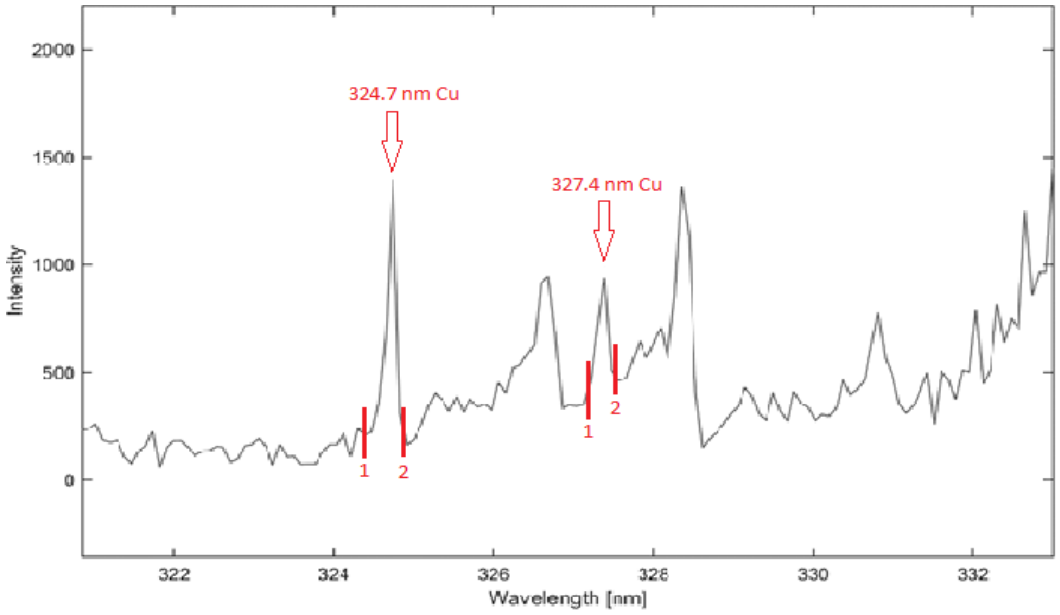


**Figure 2.1 Selected portion of an acquired spectrum obtained during Cu emission showing the 324.7 and 327.4 nm wavelength peaks.**

Background correction was accomplished by subtracting the integrated background signal from the integrated emission peak. When signal to background ratios (SBR) were assessed, the background used was the mean of the signal of the wavelengths used for calculation of the integrated signal, averaged over a period of time, X. The signals in the SBR calculations were the highest signal intensities across the selected wavelength range, averaged over a time equal to X. Signal to noise ratios (SNR) were calculated using transient signals of discrete 50 µL injections. The averaged standard deviation of the same wavelength selection pre- and post- analyte injection was used to define the noise in the system. The integration of the signal of the analyte injection response was used as the signal. Limits of detection (LOD) were calculated using the same transients. LODs were assessed using the method of calculation outlined in the following equation[41]:

$$LOD = \frac{(\mathrm{k} \times \sigma_{bl} \times \mathrm{C}_s)}{(\mathrm{S} - \mathrm{S}_{bl})}$$

In these calculations, the constant k is set to 3, indicative of a 95% confidence level, $\sigma_{bl}$ represents the standard deviation of the background signal, $C_s$ is the concentration of the sample in µg $mL^{-1}$, S represents the total analyte signal intensity, and $S_{bl}$ is the average intensity of the background signal.

*Sample Preparation*

Ten analytes were selected for evaluation based on three specific differentiators: 1) previous use in plasma characterization, 2) variance in chemical characteristics, and 3) diversity of possible future in-field applications for this emission source. Each of the analyte stock solutions was prepared in 2% $HNO_3$ from their nitrate salts ((purity> 99.999 %) $LiNO_3$ and $Mg(NO_3)_2 \cdot 6H_2O$ (GFS Chemicals, Inc., Powell, OH, USA), $AgNO_3$ and $Pb(NO_3)_2$ (Sigma-Aldrich Inc., St. Louis, MO, USA)) or diluted from 1000 ± 3 µg $mL^{-1}$ standards in 2% $HNO_3$ (Na, Cu, Zn, As, Cs, and U (High Purity Standards, Inc., Charleston, SC, USA)). The final solutions were generated to be single element solutions of 500 µg mL-1 in 2% $HNO_3$.

**Results and Discussion**

Before certain figures of merit and elucidation of underlying mechanisms of a novel instrument are able to be fully investigated, it is imperative to select spectral lines with high signal-to-noise ratio (SNR) and signal-to-background (SBR) values. Consistent use of the same methodically selected lines supplies a better evaluation of the method by assuring consistent comparisons as development continues, increasing confidence and the ability to assess reproducibility of the instrumentation.

Evaluation of potential analytical lines was systematically completed for each element by exploring the full spectral emission (signal intensity versus wavelength) from 190 - 884 nm for a 500 µg $mL^{-1}$ single element solution injected into a continuous flow of 2% $HNO_3$ to observe and record the emission line response corresponding to that element. The use of such high test solution concentrations allowed for linear emission response with changes in concentration for a broad range of spectral line intensities. It is important to note that previous study has indicated that the source behaves more spectroscopically like a flame than an ICP source[26], meaning that electronic transitions statistically viable for analysis are more similar in regards to the intensity proportions found in flame-type emission sources, i.e. the presence of more atomic than ionic transitions. Discrete injections of each solution were repeated three times to collect time-dependent data of the analyte emission response in the plasma to assess the practical measurement metrics, an example of which is shown in Fig. 2.2. The data from these experiments was evaluated by comparison of calculated values such as signal-to-noise, signal-to-background, and theoretical LOD as outlined in the Experimental section above for uniform evaluation.

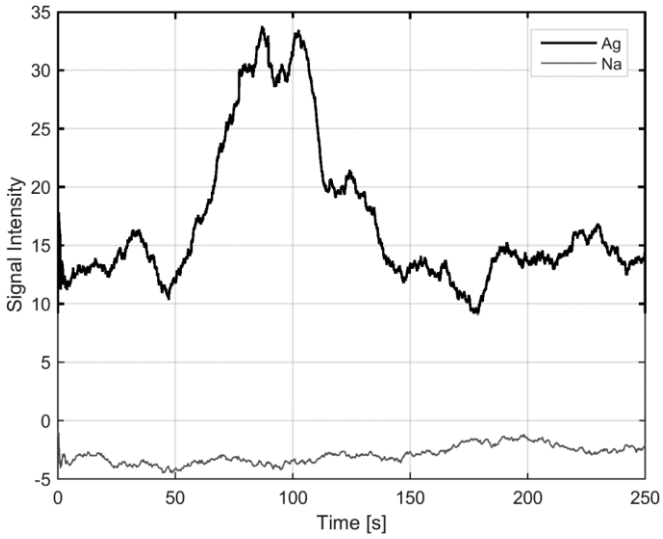


**Figure 2.2 Emission signal intensity over time in seconds of a 50 µL injection of 500 µg $mL^{-1}$ Ag (328.1 nm) into a continuous stream of 10 µg $mL^{-1}$ Na (588.9 nm) in 2% $HNO_3$.**

Displayed in Fig. 2.3 is a representative emission spectrum of a multi-analyte 50 µL injection containing Mg and Ag, each at 500 µg $mL^{-1}$. He emission is a prominent contributor to the background spectra as would be expected using an emission source sheathed in He gas. Other background species consistently present in the emission spectra include NH, OH, and $N_2$. These molecules are present due to the electrolytic solution used to sustain the plasma (i.e. $H_2O$ and $HNO_3$) and due to the atmospheric species as this is an emission source which operates in ambient conditions, (e.g. $N_2$).

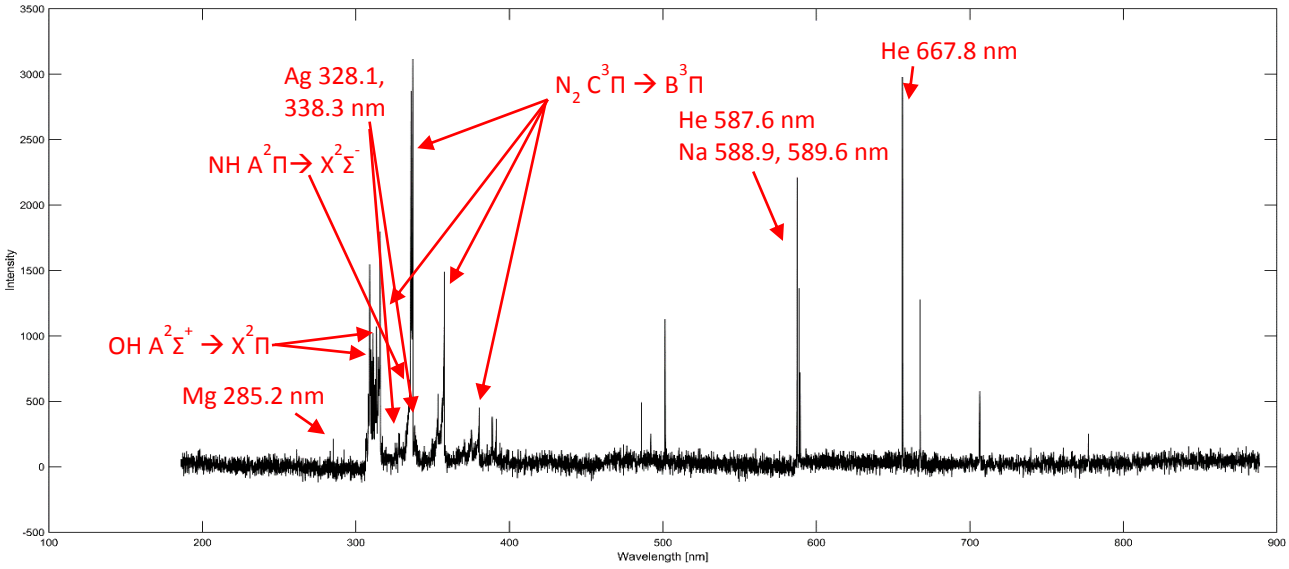


**Figure 2.3 Typical multi-element spectrum including Mg, Ag, Na, with background molecular emission bands of OH, $N_2$, and NH.**

Though not yet researched through rigorous experimentation, it is apparent that adjusting the optical components to favor selected areas of the plasma emission enhances the signal-to-background ratio by reducing the contribution of the background emission. As an example, notice the difference in He line emission intensity between Fig. 2.3 and Fig. 2.4 at wavelengths 587.6 and 667.8 nm in comparison to the intensity of the OH and $N_2$ molecular emission bands. Region-specific emission within the plasma means that

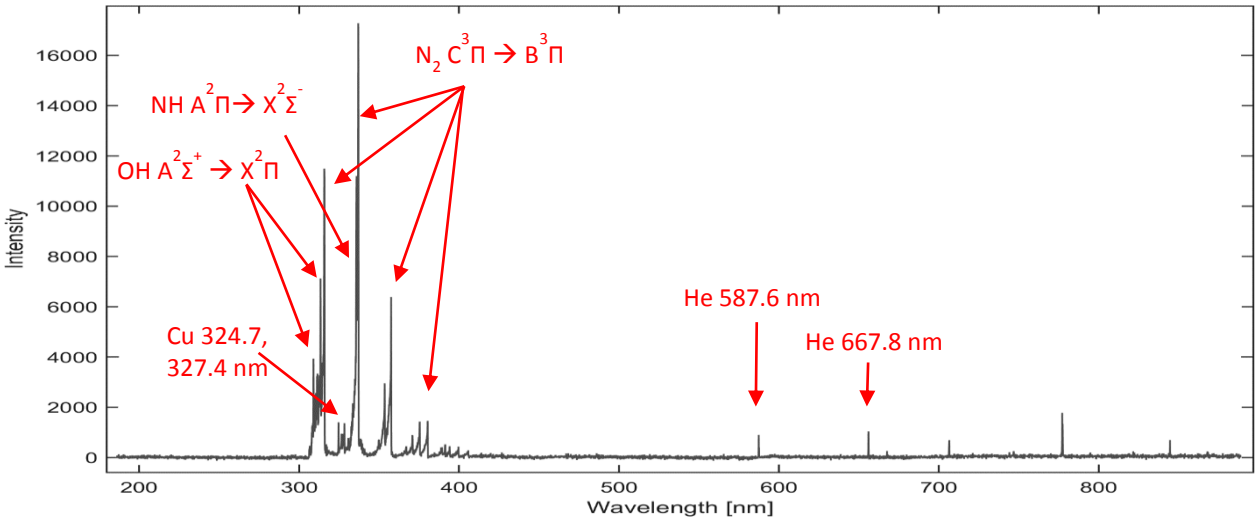


**Figure 2.4 Spectrum of Cu emission during 50 µL injection at lines 324.7 and 327.4 nm**

optically focusing on different depths of the plasma, or observing the emission from different physical positions, allows for biasing detection against either $N_2$ and OH molecular bands (indicating emission from ambient air and the water from the electrolytic solution suggesting that the area where the sample is being delivered is in optical focus) or alternatively He (indicating observation of the emission of the sheath gas of the plasma suggesting the external surface of the plasma is in focus). Due to this, 10 µg $mL^{-1}$ Na was used as an internal standard within the constantly flowing 2% $HNO_3$ at 150 µL $min^{-1}$. Using Na as an internal standard ensured optically focusing on the plasma in areas where analyte emission occurrs while minimizing contributions from the background species. Na was chosen as the internal standard due to its responsiveness and the spectral proximity of 589.0 nm emission to a prominent background line, He 587.6 nm as seen in Fig. 2.3. The spectral location of the internal standard at the middle of the spectral range minimizes the effects of chromatic aberration by focusing the wavelength range on to the fiber optic cable for optimal signal detection. During the analysis of the Na emission lines

as analytes, Ag was added to the continuous $HNO_3$ flow as an internal standard. This selection was made as Ag has a correlated signal response to Na in the sense that is has a quick response to changes in concentration as well as fluctuations in the LS-APGD[27] and emits spectrally close to background lines (e.g. $N_2$ $C^3\Pi \rightarrow B^3\Pi$ in the region 300-400 nm) as seen in Fig. 2.3. Using an element that emits at a wavelength close to that of the background signal as the internal standard ensures that any changes in the ratio of signal intensities of the analyte to background can be attributed to source variance, not chromatic aberrations.

As seen in Fig.2.2, the transient responses for each analyte, both the emission of the analyte of interest and the internal standard, Na, can be plotted to provide a visualization of the injection made. The emission signal of Na over time during the injection remains consistent, indicating that there was no significant change in the plasma power density upon sample introduction. One might imagine a change in the distribution of energy in the plasma (e.g. increased current, decreased liquid flow, etc.), but this is not seen. The transient signal seen is not a smooth ascending and descending peak, but has a reproducible anomaly on the decent around 115 seconds. This secondary increase in signal is thought to be from the analyte adsorbing to the counter electrode, only to volatilize and re-emit later. This can be seen by the elemental surface analysis of a used LS-APGD electrode in Appendix 1. This is not seen for all elements, and a future evaluation into the characteristics of peak shape is recommended for comparison with elemental melting temperatures and likelihood to remain on the LS-APGD source components. Given the lens positioning to optimally collect all emission light, secondary

emission from an analyte on the counter electrode may be collected and artificially increase the signal after the injection. The signal-to-background, signal-to-noise, and LOD characteristics were calculated from these transient responses. Looking to the data in Table 2.1, the previously mentioned adsorption is hypothesized to be a significant contributor to the large relative standard deviations (RSD) in the transient signals. The RSD in Table 2.1 is a measurement of the deviation in signal intensities collected over multiple injections. The non-uniform adherence of analyte to the counter electrode would provide significantly non-uniform reproducibility between injections.

Table 2.1 summarizes several practical measurement metrics across the ten evaluated analytes. Two columns containing wavelengths are listed, labelled 'Lines Monitored (nm)' and 'Wavelengths Evaluated (nm)'. The wavelengths of lines listed in the prior column are the lines of highest spectral intensity within each element's specific set of emission lines[29]. The wavelengths selected for evaluation were those with signal-to-noise ratios greater than 100 for injections of 500 μg $mL^{-1}$ single element solutions, except in the cases of Cs and U, in which the wavelength which produced the highest signal-to-noise ratio was selected. Analytes of different species are expected to present different emission line intensities, based on transition probabilities[40]. Evaluation of the intensity of emission from various elements provides insight to the microplasma environment as it corresponds to emission. The total intensity of emission in a spectral line (i.e. area under the curve to account for spectral broadening) of a particular frequency per unit volume of emission source is proportional to the individual atomic transition probability as well as the number density of excited atoms in the upper energy

level[40]. Many of the analyte responses align with the expected emission intensity of the elements evaluated, such as Cu (transition probability 1.39 $10^8$ $s^{-1}$) having a higher LOD and lower signal-to-noise ratio than Ag (transition probability 1.30 $10^8$ $s^{-1}$). It can also be noted in Table 2.1 that ionic state atoms see a poorer emission response than the neutral atoms. The transition probability of ionic states is lower than that of neutral atoms from the increased effective nuclear charge on the outer electrons of these cations[40]. One reason for the poor detection of the easily ionizable elements, such as Cs, could be due to a high likelihood of ionization within the plasma, entering a state with lower transition probability, and therefore less detection.

The limits of detection (LOD) as calculated by the method outlined in 'Experimental: Spectral data processing' are listed in Table 2.1. The LODs for even the least responsive of elements are on the order of mg $L^{-1}$. Comparing to another electrolytic solution glow discharge source such as the miniature Solution Cathode Glow Discharge (SCGD) designed by Hieftje and coworkers[42], the LS-APGD produced higher LODs on the scale of mg $L^{-1}$ compared to SCGD LODs of 0.2-270 µg $L^{-1}$[22]. One large contribution to this difference lies in the detector used for emission analysis; a more sensitive PMT for the SCGD and a more portable CCD for the LS-APGD. Though this is not a competitive set of values in regards to many laboratory confined emission detection systems (e.g. ICP-AES, single µg $L^{-1}$ range LODs[43]), when examining the quantity of analyte needed for analysis and detection (i.e. nanograms of sample vs. concentration of analyte), it can been said that the LS-APGD is very efficient in exciting small amounts of sample; therefore, requiring less overall amount of sample for analysis. It is pertinent to mention

| *Element* | *Lines Monitored (nm)* | *Wavelength Evaluated (nm)* | *Signal-to-Background Ratio* | *Signal-to-Noise Ratio At 500 µg mL$^{-1}$* | *RSD of Transient Signal (%)* | *Estimated Limit of Detection (µg mL$^{-1}$)* | *Equivalent mass required for analysis (ng)* | *Ratio to Internal Standard* |
|---|---|---|---|---|---|---|---|---|
| *Li* | I: 610.4, 670.8 | 610.4 | 10.8 | 178 | 10 | 0.66 | 33 | 28.8 |
| | | 670.8 | 55.0 | 999 | 8.6 | 0.09 | 5 | 34.9 |
| *Na* | I: 589.0, 589.6 | 589.0 | 26.0 | 741 | 9.9 | 0.19 | 10 | N/A |
| | II: 328.6 | 589.6 | 24.6 | 698 | 12 | 0.21 | 11 | N/A |
| *Mg* | I: 285.2 | 285.2 | 2.4 | 120 | 16 | 3.59 | 179 | 23.5 |
| | II: 279.6, 280.3 | | | | | | | |
| *Cu* | I: 324.7, 327.4 | 324.7 | 2.6 | 196 | 28 | 1.55 | 78 | 18.6 |
| | II: 224.7, 368.7, | 327.4 | 2.1 | 135 | 24 | 3.54 | 177 | 17.3 |
| | 491.0, 780.8 | | | | | | | |
| *Zn* | I: 213.9, 481.1 | 202.6 | 152.5 | 550 | 17 | 0.54 | 27 | 18.7 |
| | II: 202.5, 206.2, | 206.2 | 57.1 | 489 | 19 | 0.81 | 41 | 10.0 |
| | 210.0, 255.8 | 213.9 | 143.1 | 516 | 17 | 0.58 | 29 | 17.7 |
| | | 481.1 | 61.0 | 220 | 21 | 1.15 | 58 | 11.6 |
| *As* | I: 286.0, 278.0 | 286.0 | 71.2 | 229 | 28 | 1.29 | 65 | 6.8 |
| | II: 449.4, 450.8 | | | | | | | |
| *Ag* | I: 328.1, 338.3 | 328.1 | 196.3 | 683 | 11 | 0.15 | 8 | 19.3 |
| | II: 241.3, 243.8 | 338.3 | 86.2 | 311 | 14 | 0.33 | 17 | 15.3 |
| *Cs* | I: 852.1 | 852.1 | 2.1 | 58 | 47 | 11.6 | 580 | 4.2 |
| | II: 460.4, 522.7 | | | | | | | |
| *Pb* | I: 405.8 | 405.7 | 44.4 | 160 | 53 | 1.92 | 96 | 6.2 |
| | II: 220.4 | | | | | | | |
| *U* | I: 358.5 | 358.5 | 1.4 | 7 | 69 | 76.33 | 3816 | 2.7 |
| | II: 367.0, 386.0 | | | | | | | |

that the LS-APGD is more compact and does not require as many consumables or the presence of a waste reservoir as required by other instrumentation approaches (e.g. ICP-AES).

While efforts were taken to minimize chromatic aberration, such as the use of a $CaF_2$ lens, optically tuning to an analyte in the center of the spectrum to have as much of the collected spectrum in focus as possible, it is apparent that chromatic aberration cannot be fully eliminated without the use of a mirror. In efforts to achieve better LODs for the elements on the spectral edges, separate optical tuning for individual elements at the focal convergence of their precise wavelengths is recommended. U was also shown to have a

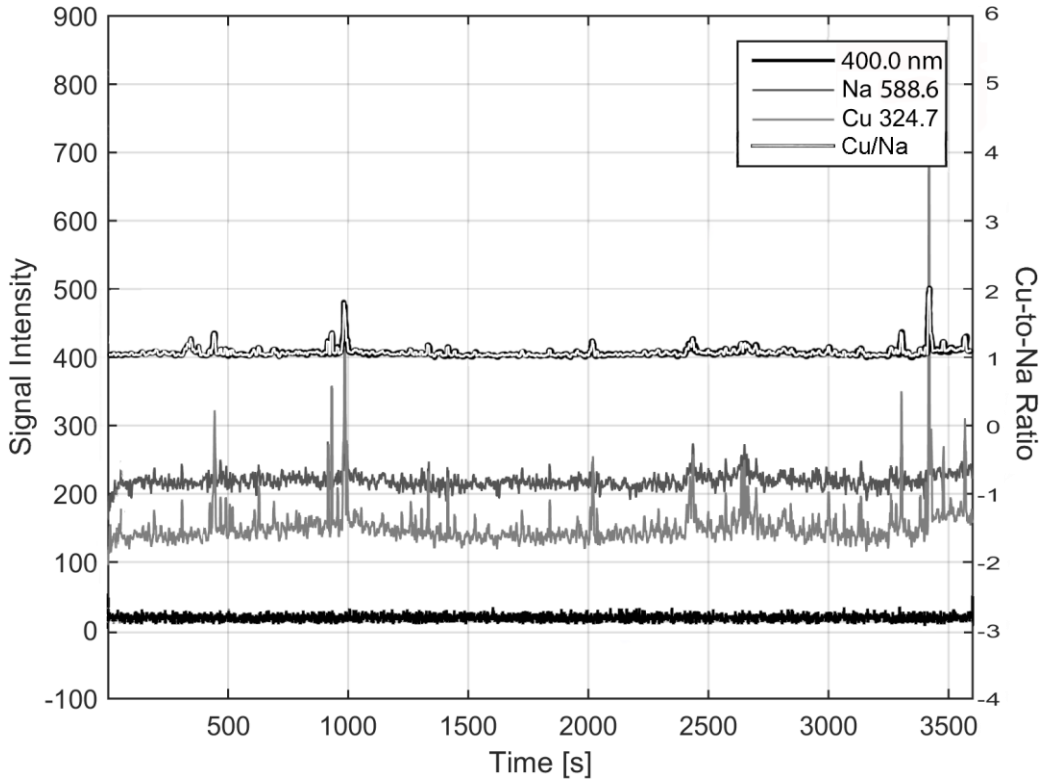


**Figure 2.5 Emission over 1 hour (3600 shots at 1 shot per second) of analytes Na 588.9 nm, Cu 324.7 nm, and background where no analyte is present (400.0 nm) corresponding to the y-axis on the left side, overlaid of a graph of the Cu-to-Na signal ratio corresponding to the y-axis on the right side.**

higher than expected limit of detection. The wavelength at which U is best observed, 358.5 nm, can experience interference in conditions with high emission from the $N_2$ $C^3\Pi \rightarrow B^3\Pi$ emission band. Atomic analyte signal may also be lost by generation of oxide molecules (e.g. $UO_2$), limiting the effective emission of the complete amount of U introduced.

More information can be derived from theoretical calculations of LODs than just a quantity of sample that is required for adequate signal acquisition. While conventionally the LOD is defined as the analyte concentration which yields a net analyte signal three times greater than the standard deviation of the background[12], this value is a combination of many physical manifestations including, but not limited to, source flicker noise, photon shot noise, and dark current shot noise. In addition to using an internal standard for ensuring the optimal collection of optical signal, the internal standard may be used to calculate a ratio of analyte signal to reference signal, eliminating much of the noise that is responsible for effecting samples uniformly. As seen in Fig. 2.5, there is a small, but significant deviation in the acquired emission signal from the microplasma over time. An aspect of this deviation can be attributed to the deviation in the amount of light collected by the spectrometer over time. This detection deviation can be seen in Fig.2.6, which shows ambient light collected over time without influence from the plasma emission. Of the two wavelengths monitored, 200.0 and 500.0 nm, the standard deviation was shown to be 0.87 (8.2%) and 1.50 (7.2%) respectively. Emission signal collection during experimentation occurs in ambient conditions, not closed within a dark room, and is subject to light noise from the sun, room light, and other stray light during

experimentation which contribute significantly to this detection deviation. In Fig. 2.5 the relative standard deviation (RSD) of the signal over a one hour time period was 15.38 % for Cu monitored at 324.7 nm, 6.22% for Na monitored at 589.0 nm, and 4.30% for an area of the spectrum selected and monitored in which no analyte was determined to be present, 400.0 nm. This time period was selected for long term signal analysis as it is significantly longer than required sample analysis time for a set of analytes. The light collection at 400.0 nm is a representation of the fluctuation in signal collection during experimentation (from sunlight, room light, computer screen, etc.). This wavelength, 400.0 nm, was chosen to monitor because no analytes which emit at this wavelength are purposefully introduced. While 15.38% is a large deviation for an analyte signal over the course of time, the average plasma signal appears consistent. This plasma variation is thought to be due to a number of factors including, but not limited to, minute fluctuations in voltage of the plasma, instabilities in the plasma hydration due to sample introduction and vaporization

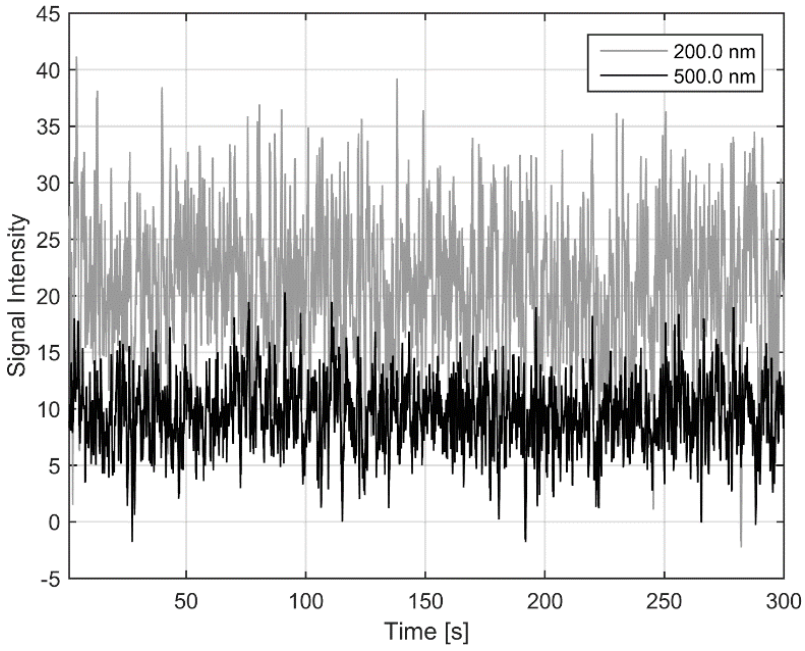


**Figure 2.6 Detection over 1 hour (3600 shots at 1 shot per second) of wavelengths 200.0 and 500.0 nm without plasma emission. Relative standard deviations of the detected signal intensity at 200 and 500.0 nm are 7.21% and 8.27%, respectively.**

rates, incomplete nebulization of high concentrations of sample, and analyte deposition onto the counter electrode post plasma residence[26]. Sample introduction has been visually observed to vary cyclically as a factor of the instability of the syringe pump feed rate.

Assuming proportional emission response from analytes, a ratio of analyte to reference signal should provide another perspective of analyte response relatively free of instability and able to normalize most plasma variations that effect all analytes equally such as sample introduction rates, voltage variations, or incomplete nebulization of liquid samples. The top line in Fig. 2.5, corresponding with the axis on the right hand side, shows the ratio of the Cu signal to the Na signal during this hour long emission collection. It is clear that a significant amount of the signal fluctuation has diminished. Some of the signal ratio variations may be due to the uncorrelated adsorption rates of the different analytes onto the counter electrode allowing for uncorrelated emissions as the adsorbed material is heated and excited from the counter electrode post initial plasma introduction.

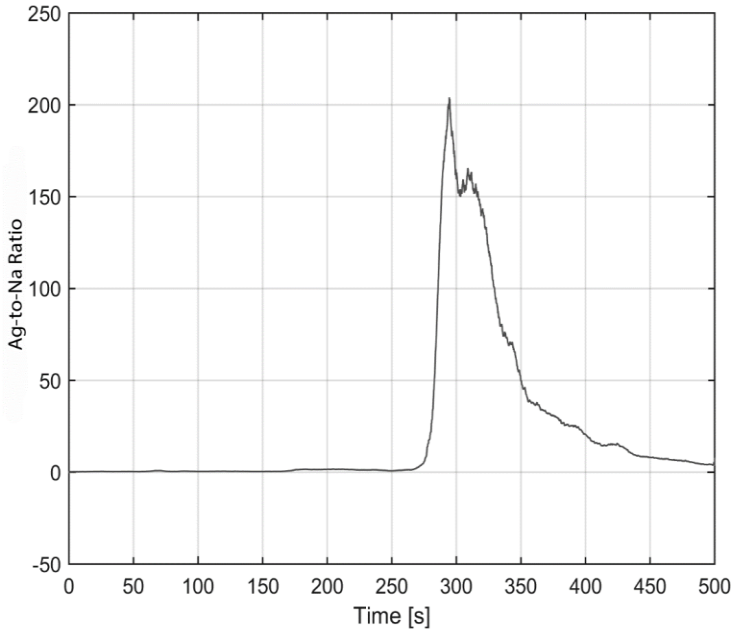


**Figure 2.7 Ratio of analyte signal to Na (588.9 nm) signal over time in seconds of a 50 µL injection of 500 µg mL$^{-1}$ Ag (328.1 nm).**

In Fig. 2.7, an analyte ratio of Ag (328.1 nm) to Na (589.0 nm) was taken throughout a 50 µL injection. When compared to Fig. 2.4, Fig. 2.7 is a much smoother

curve, indicating less standard deviation in signal acquisition. Not only does this hold promise as a method for a more robust analysis in future studies, but evaluation of a ratio to an internal standard allows for increased reproducibility in future analysis. Analytic ratios to an internal standard for future analysis of the LS-APGD as an excitation source would allow for a more reproducible comparison to be made with concern to improving the figures of merit on the path to commercialization.

**Conclusion**

A necessary set of computations for continued growth in instrumentation development of the liquid sampling-atmospheric pressure glow discharge (LS-APGD) as an excitation source was performed. Select lines were determined as the best lines to use for evaluation of the LS-APGD for ten analytes for future instrumentation experimentation as an excitation source for optical emission spectroscopy as pertains to solution introduced analytes. These selections were made through analysis of SBR, SNR, LOD, and signal ratio to an internal standard, identifying them as lines which exhibit superior calibration quality to provide higher accuracy in LS-APGD analysis.

Future studies for a deeper understanding and insight into the LS-APGD should include several different areas. First, an evaluation of analyte excitation as a factor of position in the microplasma (e.g. distance in the lateral dimension from analyte introduction to excitation, positional relation of analyte excitation to other analyte excitation, etc.) could allow for select optical focusing, eliminating the secondary emission from any anaylte adsorbing to the counter electrode. Secondly, an evaluation of matrix effects on the signal intensity of analytes and the stability of the plasma will allow

for an assessment of the source's robust emission capabilities. Additionally, further exploration into increasing reproducibility and decreasing signal deviation will be relevant to the future focus of employment of the LS-APGD as an in-field excitation source for atomic analysis.

**Acknowledgments**

This work was financially supported by the Defense Threat Reduction Agency, Basic Research Award #HDTRA1-14-1-0010, to Clemson University.

# CHAPTER THREE

# THE MATRIX EFFECTS ON DETECTION BY MEANS OF ANALYSIS BY THE LIQUID SAMPLING-ATOMSPHERIC PRESSURE GLOW DISCHARGE (LS-APGD) MICROPLASMA

## Introduction

The growing need for portable, compact chemical instruments to be used for in-field or in-line analysis is the primary motivation behind developing miniaturized optical emission spectroscopy (OES) and mass spectrometry (MS) measurement systems[11,17,44,45]. Current instruments used for elemental analysis in these methodologies are primarily resigned to the lab (e.g. ICP-MS, ICP-OES) and have seen not significant advances towards miniaturization in the past 30 years[10,46]. Inductively coupled plasma (ICP) instrumentation is resigned to stationary, in laboratory analysis due to the requirements of size, power, and consumables of both the plasma source and the accompanying spectrometers. Though the field of MS has extensive exploration towards miniaturization and portability, the prominent application of these instruments has been towards molecular, not elemental, analysis[47-49]. On-site elemental analysis, that is both qualitative and quantitative, is still in the developmental stages.

An in-field elemental analysis instrument would provide real-time results, allowing for greater time efficiency and eliminating the need to transport samples back to the lab for analysis. This is especially pertinent for samples that are unfit for postal transport due to potential hazards or unknown composition. An ideal field-capable instrument would exhibit comparable precision and accuracy to present laboratory-based

analysis as well as providing analysis over a broad linear range. A field-capable instrument must have a small footprint, require minimal power, need few consumables such as gas or solvent, and produce minimal waste to minimize the required accessory components for transport. Such an instrument must be able to operate in ambient conditions and be user friendly. Key required chracteristics include robustness and ruggedness both in terms of operational parameters and in matrix analysis. The terms robust and rugged are used here to mean "an insensitivity to changes of known operational parameters on the results" and "an insensitivity against inadvertent changes of known operational variables and in addition to unexpected variations", respectively[50]. A robust and rugged instrument in regards of matrix effects would allow for minimal sample preparation or dilution, ideal for minimizing liquids required in environments where producing minimal waste is a high priority.

Microplasmas are a prudent choice for potential portable, battery operated instruments as well as embedding in-line in existing instrumentation (e.g. an emission source for gas chromatography detection) due to their small footprint, low power requirements, and ambient environment analysis abilities[11]. Lower power requirements along with a smaller need for consumables lends itself to lower associated operating costs, ideal for in-field and embedded instrumentation. In the early 1990s, Cserfalvi et al. developed a novel microplasma for detection by OES called the electrolyte cathode atmospheric glow discharge (ELCAD)[18,51]. The ELCAD was the first design to use the electrolytic solution as the cathode, stream-lining the liquid sample introduction. This low-power ($\leq$ 75 W) source introduces the electrolytic solution through a vertically-

mounted glass tube between 2-10 mL $min^{-1}$, overflowing into a catch basin, generating a constant waterfall. An electrode suspended 3-5 millimeters above the constant stream is connected to the ground output of a d.c. power supply, sustaining a plasma between the solution surface and the counter electrode. The ELCAD sparked interest into microplasmas research as it showed microplasmas as a promising potentially portable alternative to the laboratory scale excitation and ionization sources that rely on high power inputs and high gas consumption[11].

In efforts to generate a more compact microplasma source without the catch basin of the ELCAD, the liquid sampling-atmospheric pressure glow discharge (LS-APGD) was created by Marcus and co-workers[24,25]. The LS-APGD, like the ELCAD, uses an electrolytic solution as an electrode, but introduces the solution at a low flow rate (< 300 μL $min^{-1}$) through a small capillary, sheathed in a slightly larger metal capillary delivering He gas (< 1 L $min^{-1}$) to sheath and cool the plasma. Across a 0.5-2 millimeter gap from the solution introduction capillary is a stainless steel counter electrode mounted co-linearly, sustaining a glow discharge plasma at the liquid solution surface. The LS-APGD has a low power consumption (< 50 W) but a compact size with subsequent high plasma power densities (>50 W $mm^{-3}$)[52] allowing for operation in a total-consumption mode, producing little to no waste.

The LS-APGD has been shown to meet the characteristics stated above for field-capable instrumentation including a small footprint[25], low power requirements[26], low consumables required[30], and produce little to no waste[24]. Previous operational parameter studies have shown the LS-APGD microplasma to be robust and rugged in terms of

operating capabilities[29,30,33]. Along with operational parameter versatility, the LS-APGD can be modified for optimizing sample introduction of many sample types including solid[32], liquid[52], and laser ablated particles[31].

Described here is an analysis of the LS-APGD emission source in heavy matrix conditions. Using heavy matrices samples of multiple elements, it is expected to come across interferences or detection suppression. The matrices studied here are a stout composition of solids (2.2% total solids) and a high concentration of only one element, U. By establishing the limitations of the technique in question, ways to overcome them may be found. The presented analysis of the LS-APGD of matrix effects on emission signal detection demonstrates the robustness of the source in terms of matrix effects and provides insight into future sample preparation needs.

**Experimental**

*LS-APGD source*

The LS-APGD is a microplasma generated between two electrodes, an electrolytic solution acting as one electrode delivered by a fused silica-coated metal capillary (280 mm i.d., 580 mm o.d., Restek Corporation, Bellefonte, PA, USA) and a solid stainless steel electrical feed through (304 SS, 1 kV, MDC Vacuum Products, LLC, Hayward, California, USA) functioning as the counter electrode. A continuous flow of 150 µL $min^{-1}$ 5% $HNO_3$ for analysis was maintained by means of a syringe pump (NE-1000, New Era Pump Systems, Inc., Farmingdale, NY, USA) as these flow rates have been previously determined as the optimal conditions for analysis[33]. Sample was delivered into the continuous flow by means of an injection valve (Rheodyne Manual

Sample Injector Valve 7725i, Sigma-Aldrich Inc., St. Louis, MO, USA) supplied with a 50 µL injection loop. A stainless steel capillary (316 SS, 0.8 mm i.d., 1.6 mm o.d., IDEX Health and Science, Oak Harbor, WA, USA) through which a He sheath gas (99.99% purity) is supplied is added co-axially around the solution supplying capillary. The outer metal capillary was connected to a primary gas line from the He source by means of a tee-piece (Swagelok, Solon, OH, USA) and regulated by a mass flow controller (0-1 SLPM, Alicat Scientific, Inc., Tucson, AZ, USA) at an optimal rate of 0.5 L $min^{-1}$ [33]. For emission studies the electrodes are held in a co-linear fashion (i.e. 180°) and perpendicular to the detection optics for maximum signal detection. The electrode directionality and position in respect to the spectrometer can be seen in Fig. 3.1.

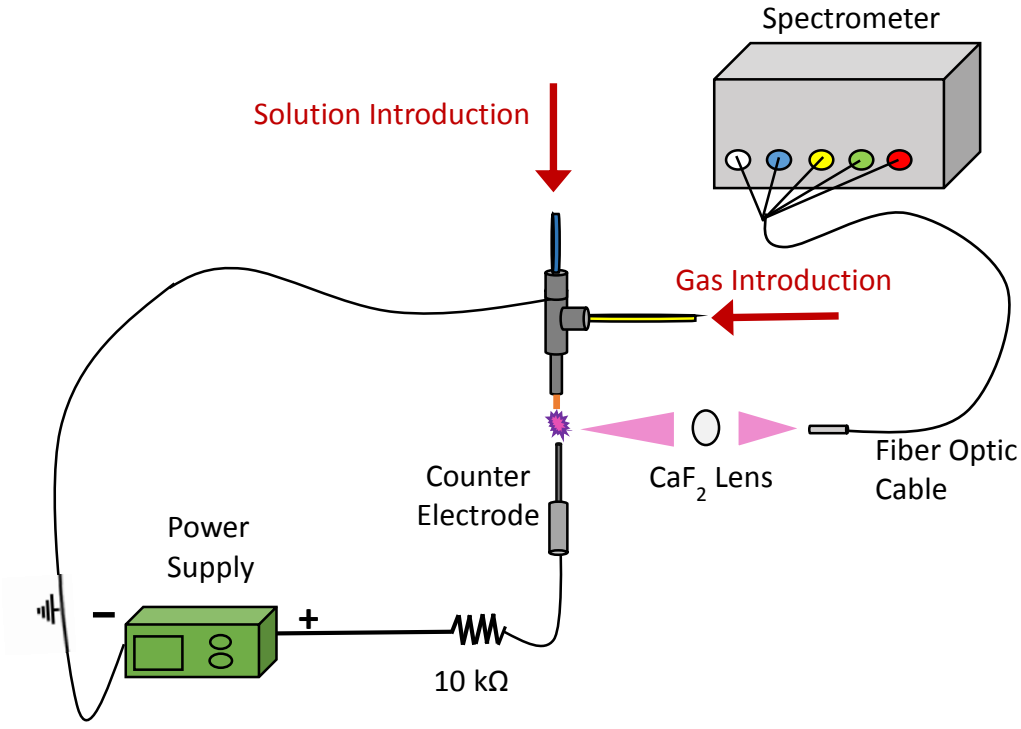


**Figure 3.1 Depiction of LS-APGD for optical emission spectroscopy. The microplasma is generated between the counter electrode and the solution capillary housed in a sheath gas electrode.**

A high voltage power supply (3 kV, 0–200 mA, SL3PN600, Spellman High Voltage Electronics Corporation, Hauppauge, NY, USA) operating in constant current mode with a negative voltage output was used to power the microplasma. A ballast resistor (10 kΩ, 300 W, Arcol Ltd UK, Truro, Cornwall, England, UK) was placed in-line between the power supply and the solution introduction electrode (anode), while the counter electrode was held at ground potential (cathode), as shown to be the most advantageous powering mode for signal collection from solution delivered analytes[26].

*Optical Emission Spectrometer*

A broad wavelength, five-channel optical spectrometer (Aurora, Applied Spectra, Inc., Fremont, CA, USA) was used for detection of the microplasma emission signal. The CCD linear array detector module within the spectrometer allows for simultaneous acquisition of 190 nm to 884 nm spectral wavelengths. A biconvex $CaF_2$ lens (25.4 mm diameter, 50.0 mm focal length, Thorlabs, Inc., Newton, NJ, USA) was used to focus the LS-APGD microplasma onto a multi-channel optical fiber bundle which collected and delivered the emission to the five separate spectrometer channels. The lens was mounted using an optomechanical cage system (Thorlabs, Inc., Newton, NJ, USA) on a translational stage (460P-XYZ, Newport Corporation, Irvine, CA, USA) to allow for optimal focusing of the microplasma emission signal entirely upon the optical fiber bundle (1:1). Data acquisition was accomplished via the 'Aurora' Data Analysis Software (Applied Spectra, Inc., Fremont, CA, USA). The software allows for collection of individual spectra (190 nm to 884 nm with spectral resolution < 0.1 nm) over a

predetermined time at an integration time of 1.05 ms and a repetition rate of 10 Hz (i.e. 1 collection every tenth of a second).

Spectra were acquired in the 'Aurora' Data Analysis Software and read into MatLab (MATLAB 8.0 and Statistics Toolbox 8.1, The MathWorks, Inc., Natick, MA, USA.) for further data processing. The integration of signal intensity over the wavelength from the onset of the emission peak until the return to baseline is the signal response at each shot. The background measurements use the same pixels for integration in the absence of the analyte. The signal response was recorded over time for 50 µL injections.

*Assessments of Limit of Detection (LOD)*

The data as visualized by a transient response seen in Fig. 3.2 was used for assessment of signal to background ratios (SBR). Limits of detection (LODs) were assessed using the SBR calculated from the transient curve data. LODs were calculated using the RSDB-SBR method as shown in the following equation[53]:

$$[LOD] = \frac{(k \times c \times 0.01 \times RSDB)}{SBR}$$

In this equation the constant k is set to 3 to indicate a 95% confidence level, c is the concentration of the sample in µg $mL^{-1}$, 0.01 adjusts the RSDB from a percentage to a ratio, and RSDB stands for the relative standard deviation of the background signal comprised of the standard deviation of the background divided by the average of the background times 100. The components of this computation are depicted in Fig. 3.2

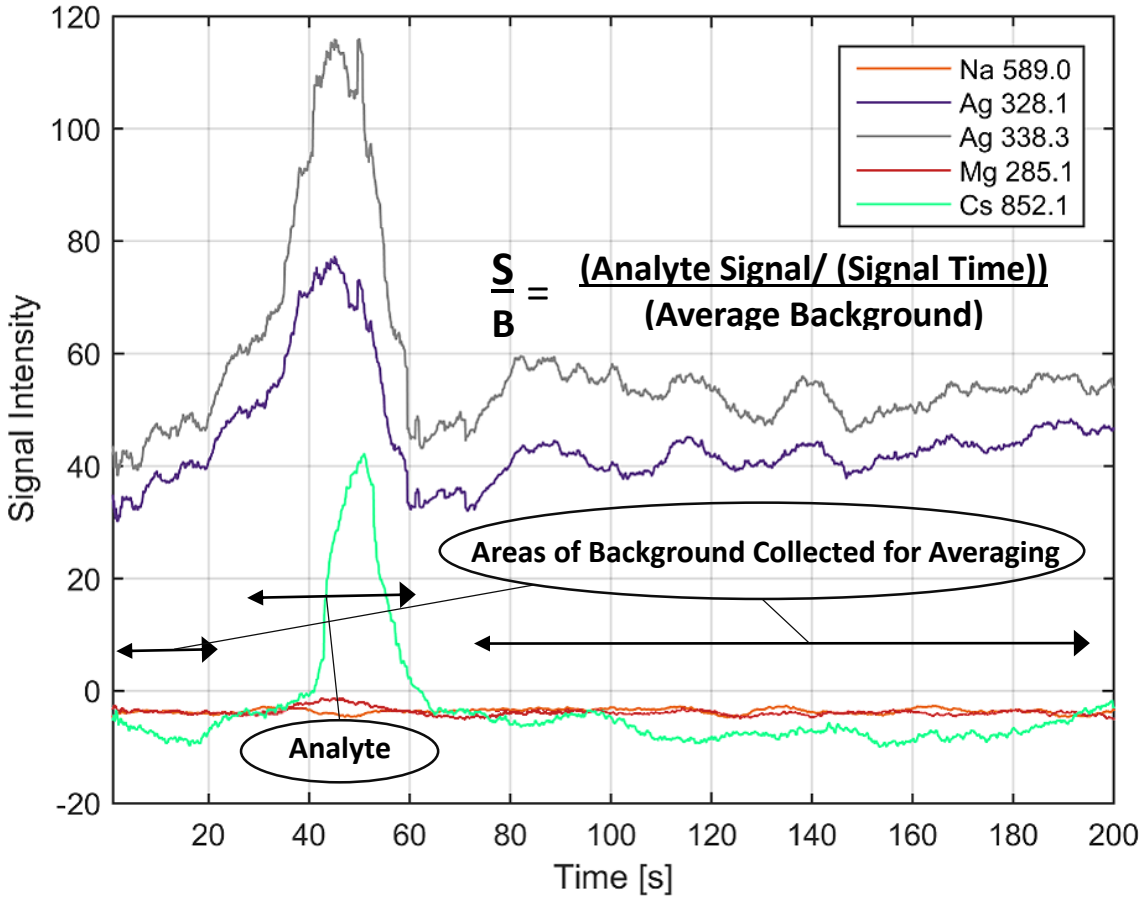


**Figure 3.2 Depiction of the methodology for assessing S/B values, and ultimately LODs, from emission peak signal responses over time**

for an injection of 500 µg $mL^{-1}$ aliquots while monitoring emission response. This calculation allows discernment of what signal can be detected with some certainty above the variations of the spectral background which corresponds to a set concentration in µg $mL^{-1}$ by using a single-point LOD method, as opposed to a calibration curve based method.

*Sample Preparation*

Consistent electrolytic solution used to sustain the plasma was 5% $HNO_3$ with 10 µg $mL^{-1}$ Na introduced to the solution from its nitrate salt (purity >99.0%) $NaNO_3$ (Sigma-Aldrich Inc., St. Louis, MO, USA) to assist in optical focusing.

Stock solutions of many elements (Al, Ba, B, Cd, Ca, Cr, C, Cu, Fe, La, Pb, Li, Mg, Mn, Ni, P, K, Re, Na, Sr, V, and Zn each at 30 µg $mL^{-1}$ in 1 M $HNO_3$ (High Purity Standards, Inc., Charleston, SC, USA)) (i.e. 2.2 % total solids/ 660 µg $mL^{-1}$ salts) and of 3 g $L^{-1}$ U in 1 M $HNO_3$ (High Purity Standards, Inc., Charleston, SC, USA)) were used as is, and at dilutions by volume of 10, 100, and 1000 times as the varied matrices of these studies. The solutions are henceforward referred to as Ref. A. and U Matrix. Mg, Ag, and Cs were added in the same concentration (500 µg $mL^{-1}$) to each of the four dilutions of both matrices to allow for consistent comparison across the range of matrices. Analytes were introduced to the 5% $HNO_3$ solution from their nitrate salts (purity> 99.99 %) $Mg(NO_3)_2 \cdot 6H_2O$ (GFS Chemicals, Inc., Powell, OH, USA), $AgNO_3$ (Sigma-Aldrich Inc., St. Louis, MO, USA) and $CsNO_3$ (GFS Chemicals, Inc., Powell, OH, USA).

**Results and Discussion**

To minimize sample handling and solvent addition in field-capable or in-line instrumentation, thereby reducing the likelihood of contamination, time needed to analyze the sample, and additional solvent to transport, it is preferable to analyze the sample without dilution or other sample preparation. In order to analyze undiluted samples, the instrument must be capable of handling heavy loads. One would expect that a high solids matrix such as Ref. A with 2.2% initial solids content would increase

stability in the microplasma, operating more stably with additional dilution. The LS-APGD plasma utilized at the conditions optimal for optical emission spectroscopy (OES) showed more stability than expected. During the triplicate 50 µL injections from 100x and 1000x matrix dilutions, the plasma did not extinguish or visibly decrease in stability. At 10x dilution from 2.2% total solids (i.e. 0.22% total solids), the plasma extinguished one time which was seen to be due to a clogged solution capillary. During undiluted Ref. A. injections, the plasma extinguished three times. This showed the decreased stability during residence times of the heavy matrix injection. Further injections of undiluted Ref. A. were done to obtain the following data. During the additional injections, 5% $HNO_3$ was injected post-sample injection. The plasma was seen to return to full stability quicker than during analysis without the 5% $HNO_3$ injections. It is thought that higher concentrations of $HNO_3$ post sample injection may additionally aid in re-stabilizing the plasma after heavy matrix injections. During injections of the U matrix and associated dilutions, no plasma extinguishes were recorded. Less stable plasma conditions were observed during injection of the undiluted U matrix as seen by minute flickering, voltage fluctuations, and inconsistencies in sample introduction, but analysis was still possible.

Matrix effects or errors are often called interference errors since they are often due to the presence of contaminants or interferents[3]. As has been previously stated, the LS-APGD source emits a spectrum more similar to that of a flame instead of an inductively coupled plasma (ICP)[26]. This means very little ionic emission is observed, as opposed to the line-rich ICP. Less ionic emission should allow for less spectral overlap in spectra observing complex samples.

The LS-APGD microplasma, like other emission sources, has a finite amount of electrical power applicable to the processes of vaporization, atomization, ionization, and excitation. It can be expected that at some concentration of total solids, the emission responses from the elements held at a constant concentration will begin to diminish. Shown below in Fig. 3.3 are the average emission responses and standard deviations for the 500 µg $mL^{-1}$ spikes of the three injections to the respective dilution factors of Ref. A. As the signal seems to increase with less dilution, it can be assumed that the upper limit of electrical power applicable to emission has not yet been met. The instability in the plasma that increases with increase in total solids percentage is shown here through an increase in standard deviation. The best repeatability between injection signal responses occurred at the 100x dilution from Ref. A. It is known that for techniques in which introduce analyte through a continuous flow, a concomitant can alter the analyte introduction and residence times, decreasing signal reproducibility[3].

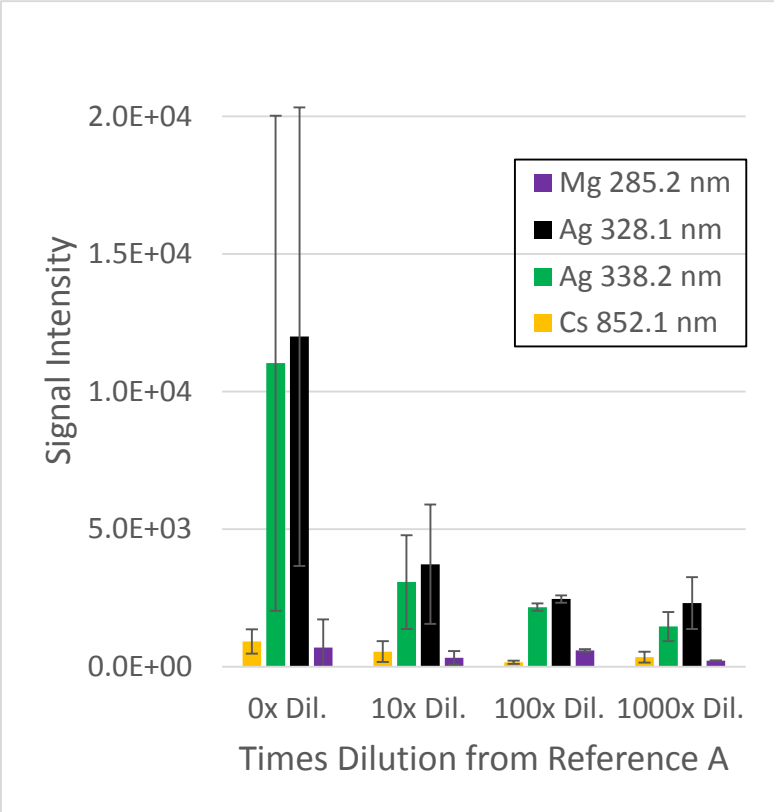


**Figure 3.3 Signal Intensities at different dilution factors from Ref. A. of 500 µg $mL^{-1}$ spikes of Mg, Ag, and Cs**

Additionally, this increased deviation supports previous plasma studies which puts emphasis on the fact that an increase in ion content, i.e. pX, allows for increase in conductivity, permitting greater stability of the discharge, independent of the identity of the ion[24]. The last two observations together indicate that the intersecting point of increasing stability due to increased ion content and decreasing stability due to increase in total percent solids can be found around 100 times dilution of Ref. A.

As stated above, and depicted in the Experimental section, limits of detection (LODs) were calculated from a single point method using signal-to-background ratios (SBR) and the relative standard deviation of the background (RSDB). Seen in Fig. 3.4 is the SBR and their reproducibility as a function of dilutions of Ref. A. As would be expected from observation of Fig. 3.3, the 0 times dilution allowed for the highest signal to background, as well as the highest deviation in the signal obtained. This is due to plasma instability as discussed earlier. The best precision is again seen at 100 times dilution. Though in the signal intensities, 100 and

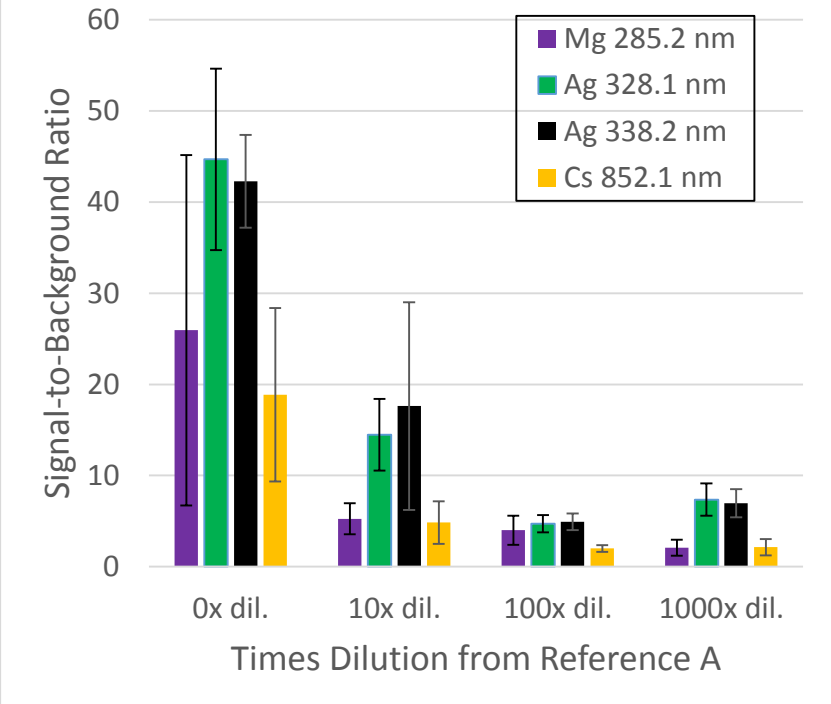


**Figure 3.4 Signal-to-background ratios and their reproducibility as a function of Ref. A. dilution factors.**

1000 times dilution factors are similar, the 1000 times dilution factor has a better SBR in most cases than the 100 times dilution factor displays. This indicates a larger background seen in 100 times dilution.

From the SBR, using the methodologies discussed in the Experimental section above, LODs at each dilution factor were calculated as seen in Table 3.1. The LODs are seen to be the best in 10x dilution from Ref. A. According to Fig. 3.3 and 3.4. the largest intensities measured are for the 0x dilution. It should also be noted that despite the high signal intensities and SBR of the 0x dilution of Ref. A., the LODs are the worst of the

**Table 3.1 Limits of detection and their reproducibility at each dilution from Ref. A.**

| Element | LOD (mg $L^{-1}$) 0x dil. | LOD (mg $L^{-1}$) 10x dil. | LOD (mg $L^{-1}$) 100x dil. | LOD (mg $L^{-1}$) 1000x dil. |
|---|---|---|---|---|
| Magnesium | 6.9 ± 3.3 | 1.6 ± 0.9 | 6.1 ± 4.1 | 5.7 ± 3.9 |
| Silver | 4.3 ± 1.4 | 2.8 ± 1.8 | 6.1 ± 3.7 | 1.5 ± 0.7 |
| Cesium | 13.7 ± 5.4 | 7.4 ± 4.6 | 10.3 ± 5.3 | 7.7 ± 5.2 |

dilution factors. This is due to the large signal deviation and continued background deviation post injection. The 10x dilution factor, with the next highest signal intensities, but much less signal deviation, provides the best LODs of samples containing Ref. A. Given the rigorous test of the system through these heavy matrices with large backgrounds, the small deviation in terms of LODs between matrix concentrations attests to the robustness of the LS-APGD. Despite the plasma instabilities obtained with the higher concentrations, capable analysis with LODs on the same order of magnitude as the

stronger diluted samples indicates the LS-APGD is capable of analysis of future samples using minimal dilution, i.e. little sample prep and less consumables.

Effects of the U Matrix on signal intensities can be seen in Fig. 3.5. 1000 times dilution of the U Matrix allowed for signal response a factor of magnitude higher than the other dilution conditions. Increase in U concentration significantly decreases emission signal intensity as well as the reproducibility of the emission signal. The common reason for U presence decreasing the signal in most optical emission spectroscopy is due to spectral interferents[54,55]. This is not the problem here given the simple atomic spectra with minimal ionic lines seen here. As U readily forms oxides, much of the finite electrical power available may be consumed through oxide formation. If not a consumption of energy problem, the presence of a larger atom, and even presence of the much larger $UO_2$ may greatly affect the residence time or sample introduction, suppressing emission signal. Whatever the cause, further investigation into the underlying signal

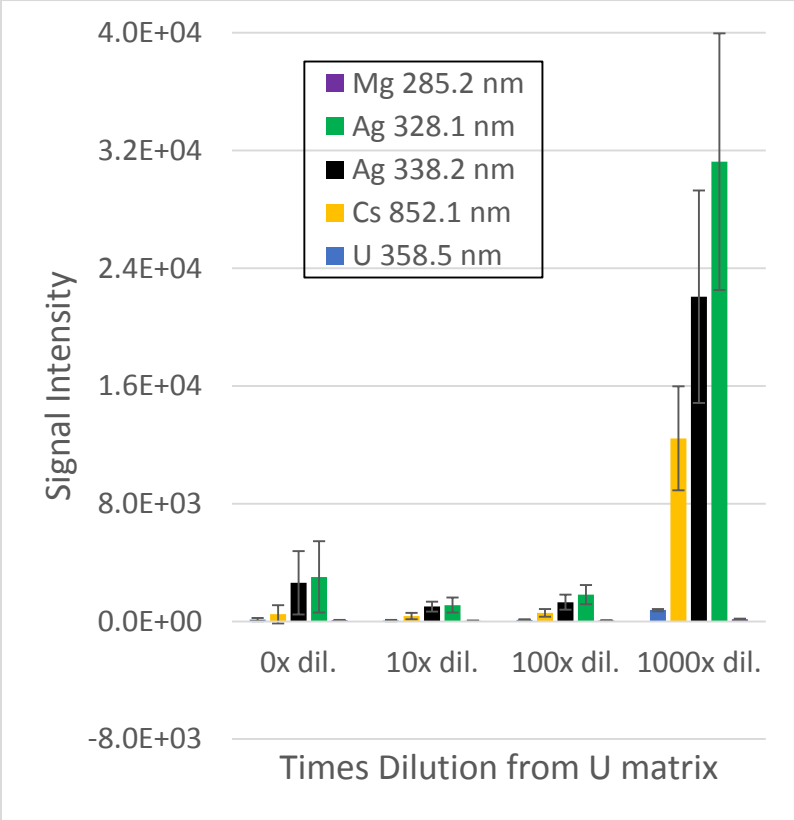


**Figure 3.5 Signal response of 500 µg mL$^{-1}$ Mg, Ag, and Cs in dilution factors of U Matrix with signal response of U.**

suppression, and other heavy matrices that may generate similar spectral effects (i.e. select f-block elements) should be carried out.

Seen in Fig. 3.6 is the SBR of the spiked analytes, as well as of U which composes the matrix. As expected, the SBR graph closely resembles the graph of signal intensities, achieving the highest values with the most dilution. The best precision of signal responses is seen at 10x dilution, but at a very low SBR. This, again, is similar to the results seen of the signal intensities. Both the signal intensities and SBR show higher values at 0x dilution of U Matrix than at 10 or 100x, but with higher deviation. These values are seen to spike to high intensities that would be expected with high concentration, but at unexpected irregular intervals. This may provide insight to sample introduction.

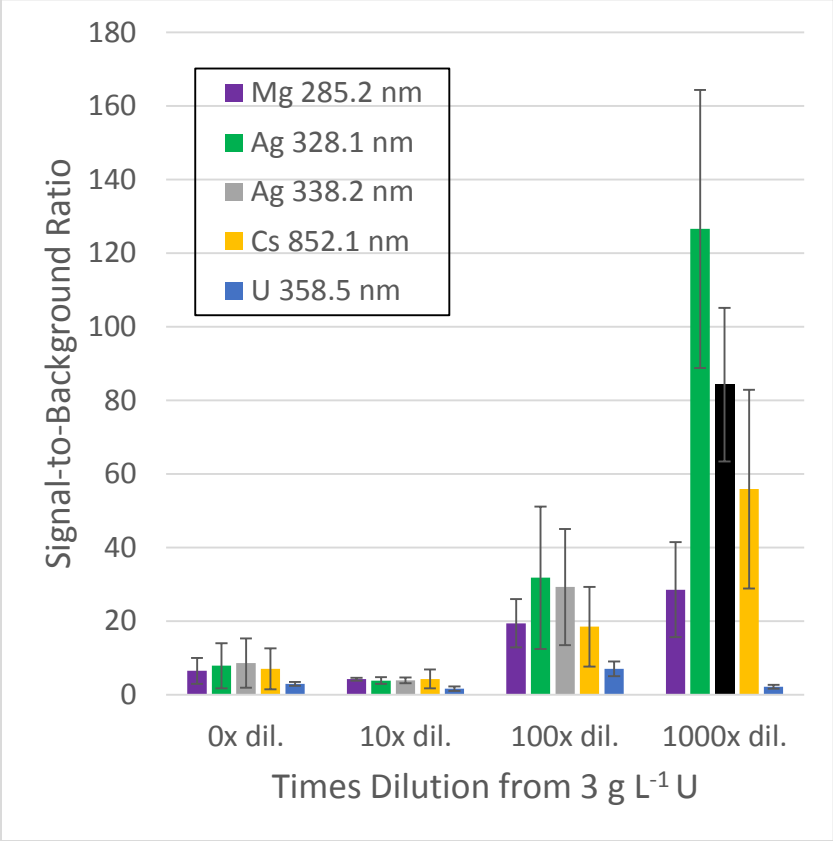


**Figure 3.6 Signal-to-background ratios and their reproducibility as a function of U Matrix dilution factors.**

Because areas of high intensities are seen, some of the large concentration is becoming introduced to the plasma, excited, and emitting. The intervals where signal suppression is

seen may be due to inadequate sample introduction as well as contributed to by inadequate excitation when U consumes the given energy to oxidize, ionize, or excite.

Using the SBR seen in Fig. 3.6 LODs were calculated for the spiked elements in the dilutions of U Matrix using the same method as discussed for dilutions of Ref. A., as seen in Table 3.2. The best LODs, i.e. the lowest concentrations, are seen at the highest dilution of U Matrix, in agreement with the signal intensity and SBR data in Fig. 3.5 and 3.6. The worst LODs of each analyte follow this same trend, agreeing with the lowest

**Table 3.2 Limits of detection and their reproducibility at each dilution from U Matrix.**

| Element | LOD (mg $L^{-1}$) 0x dil. | LOD (mg $L^{-1}$) 10x dil. | LOD (mg $L^{-1}$) 100x dil. | LOD (mg $L^{-1}$) 1000x dil. |
|---|---|---|---|---|
| Magnesium | 2.2 ± 1.0 | 10.5 ± 2.2 | 2.5 ± 0.7 | 1.6 ±0.2 |
| Silver | 8.8 ± 4.2 | 13.9 ± 6.8 | 6.2 ± 1.4 | 0.2 ± 0.1 |
| Cesium | 9.6 ± 8.2 | 54.1 ± 33.6 | 4.0 ± 1.9 | 1.7 ± 0.1 |

signal intensities and SBR at 10x dilution of U Matrix. Comparing LODs of Ref. A. to LODs of the same elements in dilutions of U Matrix, the Ref. A. dilutions show worse LOD than the analytes in U Matrix, indicating that a large amount of varied solids, and a larger concentration of matrix, generate a larger emission signal suppression for the analytes evaluated. Across all of the evaluated analytes, the lowest LOD was shown to be Ag at 0.2 mg $L^{-1}$ in the 1000x dilution U Matrix while Ag experienced the most signal suppression, as seen through the calculated LOD of 13.9 mg $L^{-1}$ in 10x dilution of U Matrix.

In the 1000x dilution of both matrices the LOD from best to worst are Ag, Mg, Cs, as in agreement with the calculated LODs provided in Chapter 2, Table 2.1, in which analysis was completed with single element solutions. At the heavier matrix conditions, this order from best to worst LOD changes. The magnitude as well as the percentage of change from best to worst LOD of each element is also different: Mg, change of 8.9 mg $L^{-1}$; Ag, change of 13.7 mg $L^{-1}$; Cs, change of 52.4 mg $L^{-1}$. These changes illustrate that the matrix effect varies between analytes. Overall, the LODs span from 0.2 mg $L^{-1}$ (Ag) to 54.1 mg $L^{-1}$ Cs. The broad range of matrix dilutions analyzed maintained analysis capabilities in the mg $L^{-1}$ concentration range.

**Conclusion**

Evaluation of the LS-APGD microplasma emission source for matrix effects indicates the ability to operate in a heavy solids composition matrix. Ideal operation occurred around 10x dilution from Ref. A. and 1000x dilution U Matrix as indicated by the signal intensities and signal-to-background ratios obtained. It is indicated that future analysis of samples should be diluted to 2.2% total solids for ideal emission response as demonstrated by the LODs obtained in Table 3.1 or to the lowest concentration of U feasible for the application as demonstrated by the LODs obtained in Table 3.2. The given LODs obtained during Ref. A. and U Matrix dilution injections indicate that if dilution of sample is not an option, the LS-APGD emission source is still capable of providing qualitative analysis with lower sensitivity. Analysis at these higher matrix concentrations requires multiple replicates to increase confidence due to a lower

precision of measurement. Continuing in the circumstance where dilution is not an option, to increase plasma stability an injection of $HNO_3$ is recommended post sample injection. In regards to U Matrix, dilution to 1000 times, i.e. 3 mg $L^{-1}$ or less is suggested to prevent signal suppression by more than an order of magnitude. Based on the studies shown, it is clear that the small footprint of the LS-APGD microplasma, its tolerance of complex matrices, and low sample/waste volumes lend themselves to suitable implementation in-field or in-line.

# CHAPTER FOUR

# CONCLUSION AND FUTURE STUDIES

This research has further characterized the liquid sampling-atmospheric pressure glow discharge (LS-APGD) microplasma as a source for optical emission spectroscopy in terms of analytical instrument capabilities. Chapter One introduced the need for field-capable instrumentation. Chapter One further included a discussion of current instruments employed for optical emission spectroscopy, a summary of the developments of the LS-APGD to date, and a description of the advantages of using the LS-APGD microplasma. Chapter Two presented a methodical approach to line selection, and established a set of limits of detection (LODs). The LODs found are $\mu g\ L^{-1}$ to $ng\ L^{-1}$ that, when combined with the small sample sizes, result in nanogram quantities of sample required for analysis. This chapter emphasized using the ratio of analyte to an internal standard to reduce signal deviation. Chapter Three investigated matrix effects on the LS-APGD including the effect on signal intensity, signal-to-background ratios, and theoretical LODs of a select set of analytes. This chapter explored matrix effects for the emission process within the LS-APGD microplasma as exhibited through detection by optical emission spectroscopy. Discussion in Chapter Three emphasized the broad range of matrices capable of being analyzed by this source. These results indicate that minimal sample preparation is required for analysis using the LS-APGD microplasma.

Since its initial development in the Marcus laboratory, the LS-APGD has shown significant promise for implementation in portable instrumentation. This research has

focused primarily on building upon the previous research on the LS-APGD microplasma; however, reaching the ultimate goal of in-field use will require additional work.

Recommended future studies include an elucidation of the underlying mechanisms behind the ionization, emission, and vaporization processes, specifically including analyte residence times within the plasma. Investigation into signal stability of analytes of interest, given the known inhomogeneities of emission within the source, an evaluation of the analyte excitation as a function of the position within the microplasma (i.e. distance in the lateral dimension from analyte introduction to excitation and relative position of excitation in comparison to other analytes) is strongly recommended, although the gains are unlikely to be worth the additional complexity.

Building upon the line selection work, a series of calibration curves followed by an assessment of certified reference materials, as well as real world samples, would illustrate the detection capabilities of a broad range of analytes of interest. To specifically build on the matrix studies, comparisons of signal response and analyte LODs in additional varieties of matrices (i.e. pH range, different percent organics, etc.), not just different dilutions of matrices, would demonstrate the ruggedness and robustness of sample analysis. These studies and more will continue to advance development of the LS-APGD and demonstrate its capability to obtain atomic and molecular information as a portable instrument.

# APPENDICES

# Appendix A

## Scanning Electron Microscopy-Energy Dispersive Spectroscopy (SEM-EDS) of Components of the Liquid Sampling-Atmospheric Pressure Glow Discharge (LS-APGD)

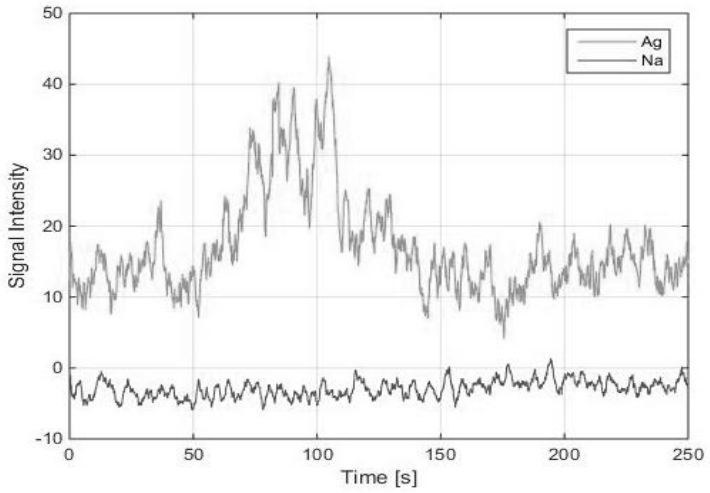


**Figure A.1: Signal intensity over time displaying a nonsymmetrical injection peak.**

In evaluations of the liquid sampling-atmospheric pressure glow discharge (LS-APGD) as an emission source, analytical data (e.g. signal-to-background, signal-to-noise, relative standard deviation of the signal, etc.) is calculated from the signal intensity collected (i.e. the integration of an emission peak over its wavelength range) with respect to time. The visualization of this data produces a transient graph, such as Fig. A.1. This graph allows for the visualization of the response of an analyte introduced at a constant rate to study the signal stability, or data collected during discrete injections of analyte, representing the change in concentration over time. When the transient graph indicates that the data has an unsymmetrical character, as seen in Fig. A.1, it is difficult to discern what physical occurrence contributes most prominently to the unexpected emission. These physical occurrences may be self-absorption, background light interference, analyte contamination, etc. When signal intensity is recorded at the

wavelength of interest a significant amount of time after the injection peak has returned to baseline (Fig. A.2) the time passed between the injection and the erratic emission, and the strength of the emission signal intensity compared to background deviations, indicate that the erratic emission is due to analyte remaining on the LS-APGD components within the region of light collection. Possible sources of analyte contamination, either from outside sources (e.g. Fe I signal leaching in overtime from the metal capillary [25]) or from analyte that remains on the LS-APGD components post plasma residence, has been theorized but not explored in depth. Presented here is a brief study using scanning electron microscopy-energy dispersive x-ray spectroscopy (SEM-EDS) to evaluate the LS-APGD components after use to explain the erratic emission signal as seen with transient graphs.

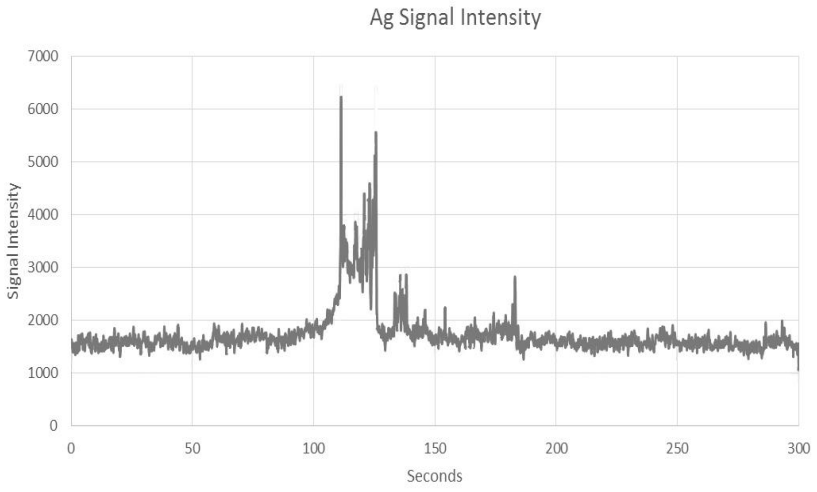


**Figure A.2: Signal intensity over time demonstrating erratic emission of the analyte of interest post-injection peak.**

SEM is traditionally used to produce magnified images of a sample. Fundamentally, the SEM operates by emitting an electron beam from a tungsten filament resulting from an application of an accelerating voltage. An energy exchange between the electron beam and the surface of the sample results in the reflection of high-energy electrons by elastic scattering, emission of secondary electrons from the sample by

inelastic scattering and the emission of electromagnetic radiation. The electron beam is rastered across the sample surface, combined with detection, to produce a distribution map of the intensity of the emitted signal. The secondary electrons emitted from the sample surface by inelastic scattering are captured by a detector during this process and projected to a television or computer monitor to produce a magnified image. This method of analysis allows for a higher spatial resolution than optical microscopy which is limited by the power of the objective lens. SEM spatial resolution is confined by the diameter and precision of the electron beam, a function reliant on the applied voltage, wavelength of the electrons, and interaction volume of the sample. Along with the secondary electrons, electromagnetic radiation, specifically x-rays, are emitted from the surface of the sample. Each element emits an x-ray specific to its unique energy characteristics. Detection of the emitted x-rays over the distribution map generated may be used to estimate the abundance of an element in a sample. This spectroscopic capability is referred to as scanning electron microscopy-energy dispersive spectroscopy or SEM-EDS[56,57].

Analysis by SEM-EDS provides powerful magnification, a large depth of field, and high resolution making it a suitable technique for analysis of the surface of the LS-APGD components. Segments of an LS-APGD microplasma source that had undergone extensive use for analysis of Ag, Cs, In, Pb, Rb, Re, Sr, and U were prepared as samples for evaluation of the adsorbtion. Samples examined with SEM-EDS must be nonvolatile, firmly mounted, electrically conductive, and grounded to prevent excess electrostatic charge accumulation at the sample surface[58]. To conform to these requirements, the front

1 inch tip of the LS-APGD counter electrode was clipped and mounted in a specimen stub before instrument introduction. The glass capilary surrounding the counter electrode during standard LS-APGD employment was also clipped and mounted on a specimen stub. To induce conductivity on the glass capillary, carbon was deposited uniformly by low-vacuum sputter coating.

Along with the SEM-EDS spectra obtained, backscattered electron imaging (BEI) and secondary electron imaging (SEI) were used to obtain images at various levels of magnifiction of the counter electrode and the glass capillary segments. BEI produces an image by detecting the high-energy electrons originating in the electron beam that have reflected or backscattered off the sample by elastic interactions. In BEI, the elements with higher atomic numbers backscatter electrons more strongly, creating a brighter pixel in the generated image than the lower atomic number elements[59] In contrast, SEI produces sample images through detection of the lower energy, inelastically scattered electrons originating within the specimen. The image contrast is generated because more of the atoms at the edge of a sample are able to escape the sample, increasing the detection and brightness to create a topographic image[59].

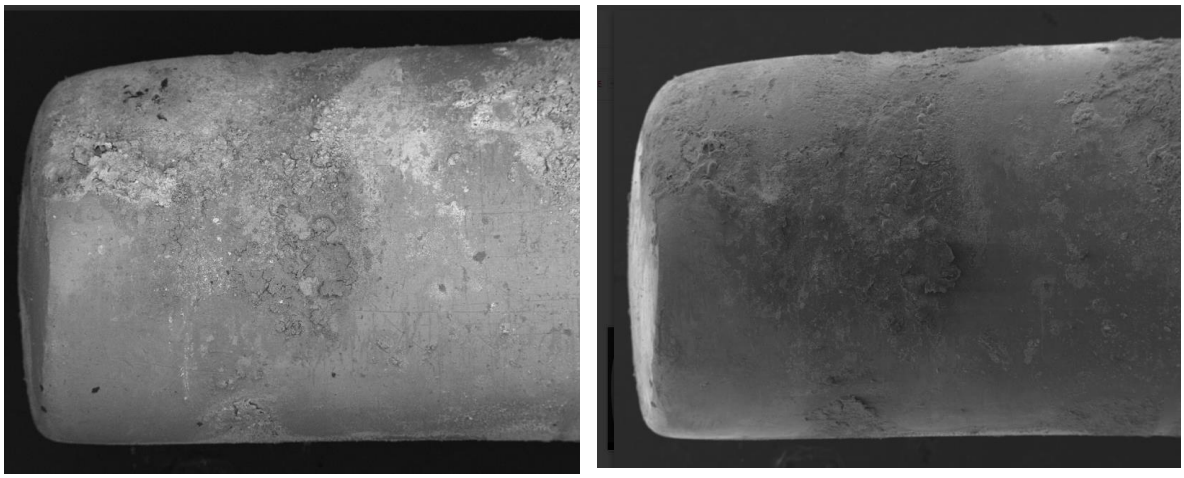

**Figure A.3 A 50x magnified image of the counter electrode tip with BEI (left) and SEI (right)**

Fig. A.3 provides an example of both BEI and SEI to provide information about the counter electrode. These images show that significant build up of multiple element masses, as seen from the light and dark regions in the backscattered image, is present post employment of the LS-APGD. The topographic image shows that the most adsorption of analyte is not at the tip where the electrode makes its connection to the microplasma, but is further up the shaft, away from the tip. A portion of this adsorption has been previously prevented from the presence of the glass capillary sheathing the stainless steel electrode. As seen in Fig. A.4, this does not prevent analyte from sticking to aspects of the LS-APGD, but it does prevent the analyte from sticking to the glass capillary. Analyte adhering to the glass capillary instead of the counter electrode may shield left behind analyte from erratic excitation and ionization post injection due to excess heat generated by the counter electrode. It should be noted that the glass capillary is slid upon the counter electrode, providing a miniscule gap, where trace analyte can be seen to reside post microplasma-introduction, as seen in Fig. A.5. Analyte becoming trapped under the glass capillary

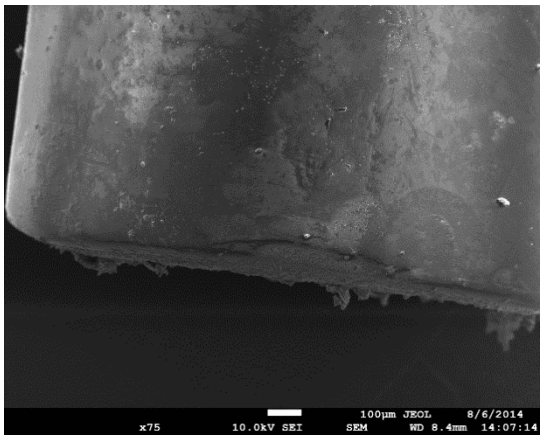


**Figure A.4 Glass capillary at 75x magnification, SEI**

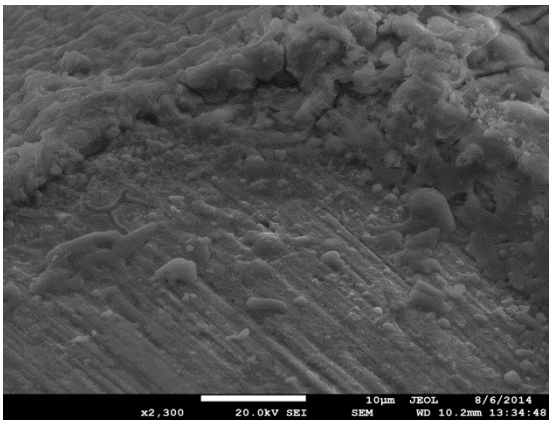


**Figure A.5 Topographic view of residue where the glass capillary had covered at 2300x magnification**

could be preventing ionized atoms from leaving the counter electrode for introduction into a mass spectrometer, but this trapped analyte may result in excited atoms remaining

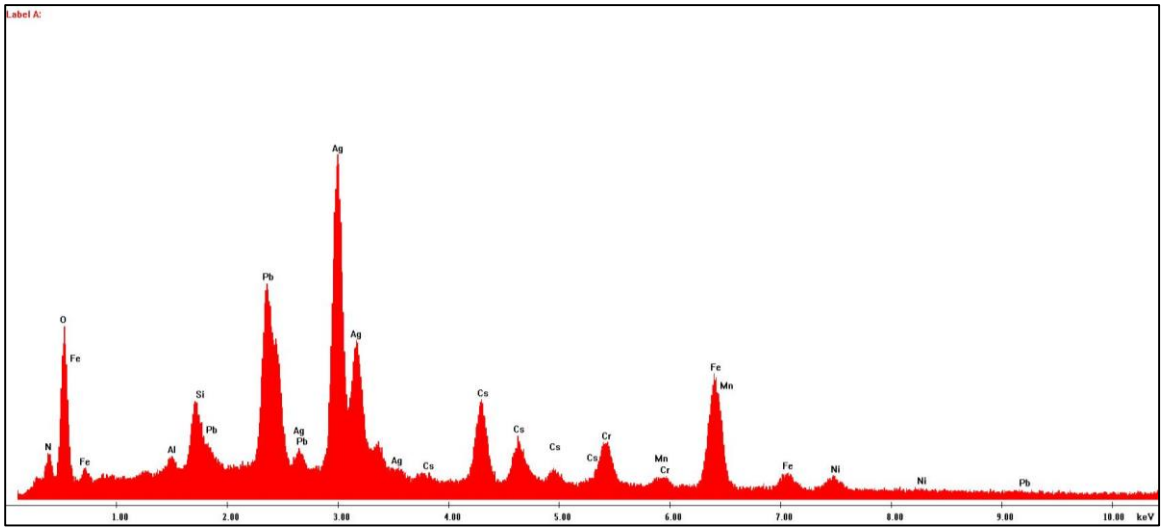


**Figure A.6 EDS spectra from counter electrode analysis identifying the surface elements**

trapped while still allowing for excitation and emission of the atoms, contributing to the unintentional erratic emission signal.

After images were obtained, the electron beam was emitted at a higher intensity to collect x-ray information for qualitative determination of the imaged residues. EDS spectra, as seen in Fig. A.6, was collected for multiple regions of the counter electrode and of the glass capillary in a variation of regions of contrast as shown by BEI.

The spectra of the counter electrode are summarized in Table A.1. The columns in the table correspond to the regions where the electron beam was focused to collect spectra. Fig. A.7 presents the general regions corresponding to the areas analyzed to generate the data shown in columns labelled 1-7 in Table A.1. Number '7', as labelled by '7 →' in the BEI image, is not shown in the image, but was spectra obtained from regions of the counter electrode that had been previously sheathed by the glass capillary. The

spectra mainly consistented of elements used during analysis using the LS-APGD microplasma: Ag, Cs, Re, and Pb. O was another prominent element, suggesting heavy formation of metal oxides in the residue.

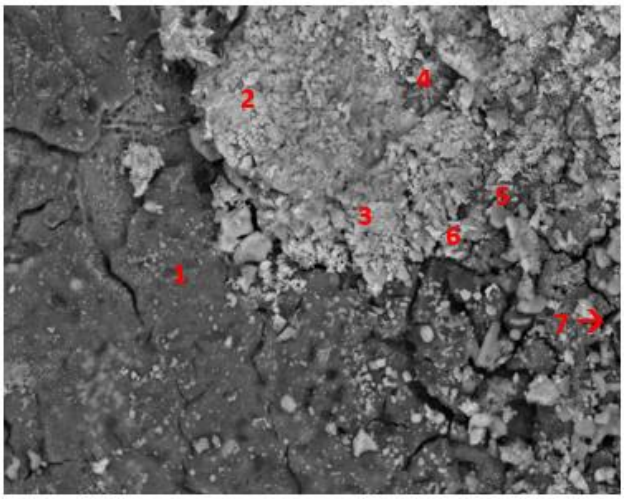


**Figure A.7: Sample image of regions of analysis and corresponding table of most frequently seen elements within the spectra by region.**

**Table A.1: Qualitative overview of the most commonly seen elements in the EDS spectra of the counter electrode**

| | 1 | 2 | 3 | 4 | 5 | 6 | 7 |
|---|---|---|---|---|---|---|---|
| **O** | **X** | **X** | **X** | X | **X** | X | **X** |
| **Si** | | | | | X | | |
| **Cr** | X | | | X | | | |
| **Fe** | X | X | X | | X | | X |
| **Ni** | X | | | | | | X |
| **Ag** | X | X | X | **X** | **X** | X | X |
| **Cs** | X | X | X | | X | X | |
| **Re** | | | | | | **X** | |
| **Pb** | X | **X** | **X** | X | **X** | X | X |

Other elements seen in this table that were frequently identified in the EDS spectra include, Fe, Cr, Ni, and Si, along with trace amounts of the elements Mn, C, N, and S. These additional elements are all components found in 304 stainless steel, the composition of the counter electrode. The elements found in 304 stainless steel that were not additionally used as analytes during use of the LS-APGD microplasma are seen less frequently, but enough that the the residue coating on the counter electrode can be called nonuniform, with some areas potentially viod of residue contamination. The Si seen in a relatively few number of analyzed locations, is thought to be contributed by the elemental presence of Si in stainless steel than from the glass capillary. It should be noted that not all of the analytes used for analysis by the LS-APGD were seen in this evaluation of the

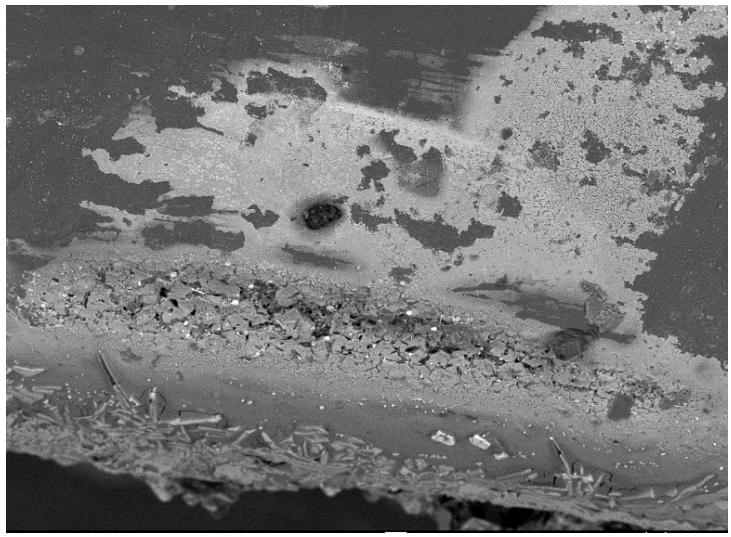

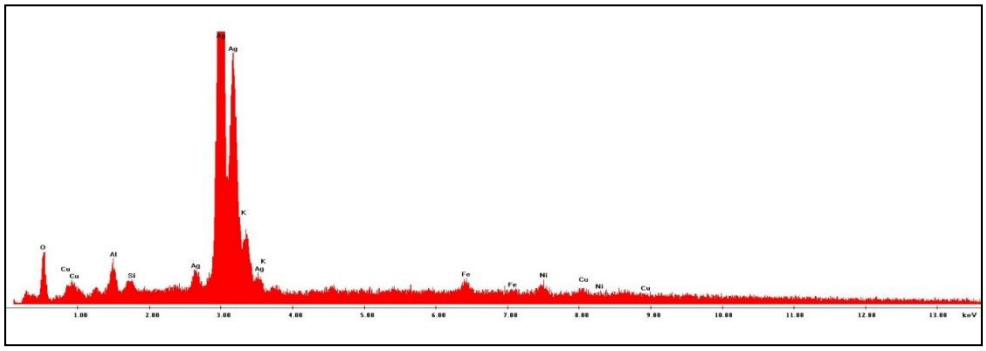

**Figure A.8 Glass capillary BEI and corresponding EDS spectra of the region.**

counter electrode as In, Rb, Sr, and U were not found on the counter electrode, nor on the glass capillary. These elements may be less prone to adsorption to the LS-APGD components, or may have just been used in lower quantities for analysis by the LS-APGD microplasma prior to EDS spectra collection.

The glass capillary showed simillar analytes as the counter electrode with a large spectral contribution from Si and O, as expected. Less expected, was the embedded residue within the front edge of the glass capillary as seen in Fig. A.8, with the associated EDS spectra resultant from positioning the electron beam on the front edge of the glass capillary, showing a significant amount of Ag present.

This analysis of the surface of an electrode used in the LS-APGD set-up emphasizes the need to clean or replace the components post-use. Over time, excessive use without removal of residue will increase contamination. Though the glass capillary does not fully prevent adsorption of analyte on the counter electrode, as shown by

column ‘7’ on Table A.1, it significantly retards the residue build up. The lack of a process to remove of residue explains a significant portion of the erratic emission signals and nonsymmetrical injection peaks, especially when using the glass capillary. With this in mind, contamination can be managed in future data collection through the development and implimentation of an electrode cleaning or replacement process between each use. Additionally, there should be an opaque glass employed to sheath the counter electrode which will minimize the erratice emission signal of analyte trapped against the counter electrode beneath the transparent glass capillary.

REFERENCES


[1] S. L. R. Ellison, V. J. Barwick and T. J. Duguid Farranr, in *Practical Statistics for the Analytical Scientist*, 2nd ed., Cambridge, The Royal Society of Chemistry, 2009.

[2] "ISO 3534-2:2006 Statistics-- Vocabulary and Symbols-- Part 2: Applied Statistics," International Organization for Standardization , Geneva, 2006.

[3] J. D. Ingle, Jr. and S. R. Crouch, Spectrochemical Analysis, Upper Saddle River, New Jersey: Prentice-Hall, Inc., 1988.

[4] K. Zhao, M. Penkin, C. Norman, S. Balsley, K. Mayer, P. Peerani, C. Pietri, S. Tapodi, S. Tsutaki, M. Boella, G. Renha Jr. and E. Kuhn, "International Target Values 2010 for Measurement Uncertainties in Safeguarding Nuclear Materials," International Atomic Energy Agency-Department of Safeguards, Vienna, 2010.

[5] W. Wardencki, R. Katulski, J. Stefański and J. Namieśnik, "The State of the Art in the Field of Non-Stationary Instruments for the Determination and Monitoring of Atmospheric Pollutants," *Anal. Chem.,* vol. 38, no. 4, pp. 259-268, 2008.

[6] C. S. Patterson, L. C. McMillian, C. Longbottom, G. M. Gibson, M. J. Padgett and K. D. Skeldon, "Portable optical spectroscopy for accurate analysis of ethane in exhaled breath," *Measurement Science and Technology,* vol. 18, no. 5, pp. 1459-1464, 2007.

[7] D. A. Cremers, A. Beddingfield, R. Smithwick, R. C. Chinni, C. R. Jones, B. Beardsley and L. Karch, "Monitoring Uranium, Hydrogen, and Lithium and Their IsotopesUsing a Compact Laser-Induced Breakdown Spectroscopy (LIBS) Probe and High-Resolution Spectrometer," *Society for Applied Spectroscopy,* vol. 66, no. 3, pp. 250-261, 2012.

[8] O. T. Butler, R. Clough, J. E. Cook, E. H. Evans, S. J. Hill, A. Taylor, M. West and A. S. Fisher, "Current trends: a perspective from 30 years of Atomic Spectrometry Updates," *J. Anal. At. Spectrom.,* vol. 31, pp. 32-34, 2016.

[9] Q. He, Z. Zhu and S. Hu, "Flowing and Nonflowing Liquid Electrode Discharge Microplasma for Metal Ion Detection by Optical Emission Spectrometry," *Applied Spectroscopy Reviews,* vol. 49, no. 3, pp. 249-269, 2014.

[10] H. E. E., J. Pisonero, C. M. M. Smith and R. N. Taylor, "Atomic spectrometry update: review of advances in atomic spectrometry and related techniques," *J. Anal. At. Spectrom.,* vol. 30, pp. 1017-1037, 2015.

[11] V. Karanassios, "Microplasmas for chemical analysis: analytical tools or research toys?," *Spectrochimica Acta,* vol. 59, pp. 909-928, 2004.

[12] P. W. J. M. Boumans, Inductively Coupled Plasma Emission Spectroscopy, New York: John Wiley and Sons, 1987.

[13] R. C. Richter, J. A. Nobrega and C. Pirola, Think Blank: Clean Chemistry Tools for Atomic Spectroscopy, Shelton, CT: Milestone Press, 2016.

[14] G. A. Zachariadis, Inductively Coupled Plasma Atomic Emission Spectroscopy: A Modern Multi-Element Technique for Modern Analytical Laboratory, New York: Nova Science Publishers, Inc., 2012.

[15] M. Huang and G. M. Hieftje, "Simultaneous measurement of spatially resolved electron temperatures, electron number densities and gas temperatures by laser light scattering from the ICP," *Spectrochemica Acta Part B: Atomic Spectroscopy,* vol. 44, no. 8, pp. 739-749, 1989.

[16] N. Jakubowski, R. Dorka, E. Steers and A. Tempez, "Trends in glow discharge spectroscopy," *Journal of Analytical Atomic Spectroscopy,* vol. 22, pp. 722-735, 2007.

[17] J. Franzke, K. Kunze, M. Miclea and K. Niemax, "Microplasmas for analytical spectroscopy," *Journal of Analytical Atomic Spectroscopy,* vol. 18, pp. 802-807, 2003.

[18] T. Cserfalvit, P. Mezeit and P. Apai, "Emission studies on a glow discharge in atmospheric pressure air using water as a cathode," *J. Phys. D: Appl. Phys,* vol. 26, pp. 2184-2188, 1993.

[19] Y. Liu, B. Sun and L. Wang, "Determination of Lithium Ion by Liquid-Phase Diaphragm Glow Discharge-Atomic Emission Spectroscopy," *Analytical Letters,* vol. 47, no. 8, pp. 1409-1420, 2014.

[20] J. Broekaert and K.-G. Reinsberg, "Spectrochemical analysis with DC glow discharges at atmospheric pressure," *Spectrochimica Acta,* vol. 106, pp. 1-7, 2015.

[21] L. Bencs, N. Laczai, P. Mezei and T. Cserfalvi, "Detection of some industrially relevant elements in water by electrolyte cathode atmospheric glow discharge optical emission spectrometry," *Spectrochimica Acta,* vol. 107, pp. 139-145, 2015.

[22] M. Webb, F. Andrade and G. Hieftje, "High throughput elemental analysis of small aqueous samples by emission spectroscopy with a compact, atmospheric pressure solution-cathode glow discharge," *Anal. Chem.,* vol. 79, pp. 7807-7812, 2007.

[23] M. Webb, F. Andrade and G. Hieftje, "Compact glow discharge for the elemental analysis of aqueous samples," *Anal. Chem.,* vol. 79, pp. 7899-7905, 2007.

[24] R. K. Marcus and W. C. Davis, "An atmospheric pressure glow discharge opitcal emission source for the direct sampling of liquid media," *Anal. Chem.,* vol. 73, pp. 2903-2910, 2001.

[25] W. C. Davis and R. K. Marcus, "An atmospheric pressure glow discharge optical emission source for the direct sampling of liquid media," *J. Anal. At. Spectrom.,* vol. 16, pp. 931-937, 2001.

[26] W. C. Davis and R. K. Marcus, "Role of powering geometries and sheath gas composition on operation characteristics and the optical emission in the liquid sampling- atmospheric pressure glow discharge," *Spectrochimica Acta Part B,* vol. 57, pp. 1473-1486, 2002.

[27] C. D. Quarels Jr., B. T. Manard, C. Q. Burdette and R. K. Marcus, "Roles of electrode material and geometry in liquid sampling-atmospheric pressure glow

discharge (LS-APGD) microplasma emission spectroscopy," *Microchemical Journal,* vol. 105, pp. 48-55, 2012.

[28] X. L. Zhang and R. K. Marcus, "Mass spectra of diverse organic species utilizing the liquid sampling-atmospheric pressure glow discharge (LS-APGD) microplasma ionization source," *J. Anal. At. Spec.,* vol. 31, pp. 145-151, 2016.

[29] L. X. Zhang, B. T. Manard, B. A. Powell and R. K. Marcus, "Preliminary Assesment of Potential or Metal-Ligand Speciation in Aqueous Solution via the Liquid Sampling-Atmospheric Pressure Discharge (LS-APGD) Ionization Source: Uranyl Acetate," *Anal. Chem.,* vol. 87, no. 14, pp. 7218-7225, 2015.

[30] X. L. Zhang, B. T. Manard, S. Konegger-Kappel and R. K. Marcus, "Evaluation of the operating parameters of the liquid sampling-atmospheric pressure glow discharge (LS-APGD) ionization source for elemental mass spectrometry," *Anal. Bioanal. Chem.,* vol. 406, pp. 7497-7509, 2014.

[31] C. D. Quarles Jr., J. Gonzalez, I. Choi, J. Ruiz, X. Mao, R. K. Marcus and R. E. Russo, "Liquid sampling-atmospheric pressure glow discharge optical emission spectroscopy detection of laser ablation produced particles: A feasibility study," *Spectrochimica Acta,* vol. 76, pp. 190-196, 2012.

[32] R. K. Marcus, C. Q. Burdette, B. T. Manard and L. X. Zhang, "Ambient desorption/ionization spectrometry using a liquid sampling-atmospheric pressude glow dischrge (LS-APGD) ionization source," *Anlytical and Bioanalytical Chemistry,* vol. 405, pp. 8171-8184, 2013.

[33] S. Konegger-Kappel, B. T. Manard, T. Konegger, L. X. Zhang and R. K. Marcus, "Liquid sampling-atmospheric pressure glow discharge excitation of atomic and ionic species," *Journal of Analytical Atomic Spectrometry,* vol. 30, pp. 285-295, 2015.

[34] B. T. Manard, J. J. Gonzales, A. Sarkar, X. Mao, L. X. Zhang, S. Konegger-Kappel, R. K. Marcus and R. E. Russo, "Investigation of spectrochemical matrix effects in the liquid sampling-atmospheric pressure glow discharge source," *Spectrochimica Acta,* vol. 100, pp. 44-51, 2014.

[35] A. Rios, A. Escarpa and B. Simonet, Miniaturization of Analytical Systems, John Wiley & Sons, Ltd., 2009, pp. 1-38.

[36] "Power Consumption Table," HIOX Softwares Pvt Ltd., October 2015. [Online]. Available: https://www.easycalculation.com/physics/electromagnetism/power-consumption-table.php. [Accessed 15 March 2016].

[37] G. W. F. Drake, Ed., in *Springer Handbook of Atomic, Molecular, and Optical Physics*, New York, New York: Springer Science+Business Media, 2006, pp. 186-197.

[38] D. A. Skoog, D. M. West and F. J. Holler, Fundamentals of Analytical Chemistry, 6th ed., 1992.

[39] M. R. Webb, F. J. Andrade, G. Gamez, R. McCrindle and G. M. Hieftje, "Spectroscopic and electrical studies of a solution-cathode glow discharge," *J. Anal. At. Spectrom.,* vol. 20, pp. 1218-1225, 2005.

[40] G. A. Zachariadis, "Chapter 1: Atomic Spectrometry," in *Inductively Coupled Plasma Atomic Emission Spectrometry,* New York, Nova Science Publishers, Inc., 2001, pp. 3-24.

[41] R. Foest, M. Schmidt and K. Becker, "Microplasmas, an emerging field of low-temperature plasma science and technology," *International Journal of Mass Spectrometry,* vol. 248, no. 3, pp. 87-102, 2006.

[42] P. Jamroz, K. Greda and P. Pohl, "Development of direct-current, atmospheric-pressure, glow discharges generated in contact with flowing electrolyte solutions for elemental analysis by optical emission spectrometry," *TrAC Trends in Analytical Chemistry,* vol. 41, pp. 105-121, 2012.

[43] H. E. E., J. Pisonero, C. M. M. Smith and R. N. Taylor, "Atomic spectrometry updates: Review of advances in atomic spectrometry and related techniques," *J. Anal. At. Spectrom.,* vol. 29, pp. 773-794, 2014.

[44] F. P. M. Jjunju, A. Li, A. Badu-Tawiah, P. Wei, L. Li, Z. Ouyang, I. S. Roqan and R. G. Cooks, "In situ analyss of corrosion inhibitors using a portable mass spactrometer with paper spray ioniztion," *Analyst,* vol. 138, pp. 3740-3748, 2013.

[45] T. W. T. Bristow, A. D. Ray, A. O' Kearney-McMullan, L. Lim, B. McCullough and A. Zammataro, "On-line monitoring of continuous flow chemical synthesis using a portable, small footprint mass spectrometer," *J. Am. Soc. Mass. Spectrom.,* vol. 25, pp. 1794-1802, 2014.

[46] T. Urabe, K. Takahashi, M. Kitagawa, T. Sato, T. Kondo, S. Enomoto, M. Kidera and Y. Seto, "Development of portable mass spectrometer with electron cyclotron resonance ion source for detection of chemical warfare agents in air," *Spectrochimica Acta Part A: Molecular and Biomolecular Spectroscopy,* vol. 120, pp. 437-444, 2014.

[47] D. T. Burns, K. Danzer and A. Townshend, "A Tutorial Discussion of the use of the terms "Robust" and "Rugged" and the Associated Characteristics of "Robustness" and "Ruggedness" as used in Descriptions of Analytical Procedures," *Journal of the Association of Public Analysts,* vol. 37, pp. 40-60, 2009.

[48] T. Cserfalvi and P. Mezei, "Electrolyte Cathode Atmospheric Glow Discharges for Direct Solution Analysis," *Applied Spectroscopy Reviews,* vol. 42, no. 6, pp. 573-604, 2007.

[49] J. L. Venzie and R. K. Marcus, "Micro-scale analytical plasmas for liquid chromatography detection," *Anal. Bioanal. Chem.,* vol. 381, pp. 96-98, 2005.

[50] P. W. J. M. Boumans, "Atomic emission detection limits; more than incidental analytical figures of merit! - A tutorial discussion of the differences and links between two complementary approaches," *Spectrochim. Acta Part B ,* vol. 46, no. 6-7, pp. 917-939, 1991.

[51] K. Satyanarayana and S. Durani, "Separation and inductively coupled plasma optical emission spectrometric (ICP-OES) determination of trace impurities in nuclear grade uranium oxide," *Journal of Radioanalytical and Nuclear Chemistry*, vol. 285, no. 3, pp. 659-665, 2010.

[52] A. Sengupta and V. C. Adya, " Determination of analytes at trace level in uranium matrix by ICP-AES without chemical/physical separation," *Journal of Radioanalytical and Nuclear Chemistry*, vol. 299, no. 3, pp. 2023 - 2026, 2014.

[53] K. Greenough, "Instrumental Theory," in *Forensic anlysis of cosmetic face powders*, Ann Arbor, MI, Proquest Information and Learning Company, 2007, pp. 9-17.

[54] D. E. Newbury, D. C. Joy, P. Echlin, C. E. Fiori and J. I. Goldstein, "Advanced Scanning Electron Microscopy and X-Ray Microanalysis," in *Advanced Scanning Electron Microscopy and X-Ray Microanalysis*, New York, Plenum Press, 1986, pp. 3-38.

[55] E. Reeves, "Scanning Electron Microscopy and the Analysis of Glass," in *Elemental analysis of glass via variable pressure scanning electron microscopy-energy dispersive spectroscopy (SEM-EDS)*, Ann Arbor, MI, ProQuest Information and Learning Company, 2001, pp. 7-10.

[56] J. I. Goldstein, in *Scanning electron microscopy and x-ray microanalysis*, 3rd ed., New York, Kluwer Academic/Plenum Publishers, 2003.

[57] M. R. Webb, F. J. Andrade and G. M. Hieftje, "High throughput elemental analysis of small aqueous samples by emission spectroscopy with a compact, atmospheric-pressure solution-cathode glow discharge," *Anal. Chem.*, vol. 79, pp. 7809-7812, 2007.

[58] J. L. Venzie and R. K. Marcus, "Effects of easily ionizable elements of the liquid sampling-atmospheric pressure glow discharge," *Spectrochimica Acta*, vol. 61, pp. 715-721, 2006.

[59] J. E. Sansonetti, W. C. Martin and S. L. Young, "Handbook of Basic Atomic Spectroscopic Data," National Institute of Standards and Technology, 16 September 2014. [Online]. Available: http://www.nist.gov/pml/data/handbook/index.cfm. [Accessed 12 March 2016].

[60] R. K. Marcus, C. D. Quarles, Jr., C. J. Barinaga, A. J. Carado and D. W. Kopenaal, "Liquid Sampling-Atmospheric Pressure Glow Discharge Ionization Source for Elemental Mass Spectrometry," *Anal. Chem.*, vol. 83, no. 7, pp. 2425-2429, 2011.

[61] P. W. J. M. Boumns, "UNDERSTANDING SPECTROSCOPY WITH A VIEW TO RATIONALIZING SPECTROCHEMICAL ANALYSIS - AN ABYSMAL ADVENTURE OR A REALISTIC IDEAL," *Spectrochimica Acta*, vol. 46B, no. 6-7, pp. 725-739, 1991.